ALKB-8, a 2-oxoglutarate-dependent dioxygenase and S-adenosine methionine-dependent methyltransferase modulates metabolic events linked to lysosome-related organelles and aging in *C. elegans*

Johana Kollárová[1], Markéta Kostrouchová[1,2,#], Aleš Benda[3], and Marta Kostrouchová[1*]

1 Biocev, First Faculty of Medicine, Charles University, Průmyslová 595, 252 42 Vestec, Czech Republic

2 Department of Pathology, Third Faculty of Medicine, Charles University, Ruská 87, 10000 Praha 10, Czech Republic

3 Imaging Methods Core Facility, BIOCEV, Faculty of Science, Charles University, Prague, Czech Republic

[*] Corresponding author:

Marta Kostrouchová

Biocev, First Faculty of Medicine,

Charles University,

Průmyslová 595, 252 50 Vestec,

Czech Republic

email: marta.kostrouchova@lf1.cuni.cz

Markéta Kostrouchová

Abbreviations:

AlkB – *Escherichia coli* Alpha-ketoglutarate-dependent dioxygenase AlkB

ALKBH1 – Alkylated DNA repair protein AlkB homolog 1

ALKBH8 – Alkylated DNA repair protein AlkB homolog 8 (a.k.a. ABH8)

***alkb-8* –** *C. elegans* gene coding for the orthologue of the ALKBH8

ALKB-8 – *C. elegans* ortholgue of ALKBH8

FTO – Fat mass and obesity associated protein

TRM9 – yeast TRna Methyltransferase 9, a SAM-dependent methyl transferase

SAM – S-adenosyl methionine

RNAi – RNA interference

LRO – Lysosome related organelles

RRM – RNA recognition motif

Abstract:

ALKB-8 is a 2-oxoglutarate-dependent dioxygenase homologous to bacterial AlkB, which oxidatively demethylates DNA substrates. The mammalian AlkB family contains AlkB homologues denominated ALKBH1 to 8 and FTO. The *C. elegans* genome includes 5 AlkB-related genes, homologues of ALKBH1, ALKBH4, ALKBH6, ALKBH7 and ALKBH8, but lacks homologues of ALKBH2, 3 and 5 and FTO.

ALKBH8 orthologues differ from other AlkB family members by possessing an additional methyltransferase module and an RNA binding N-terminal module. The ALKBH8 methyltransferase domain generates the wobble nucleoside 5-methoxycarbonylmethyluridine from its precursor 5-carboxymethyluridine and its (R)- and (S)-5-methoxycarbonylhydroxymethyluridine hydroxylated forms in $tRNA_{UCG}^{Arg}$, and $tRNA_{UCC}^{Gly}$. The ALKBH8/ALKB-8 methyltransferase domain is highly similar to yeast TRM9, which selectively modulates translation of mRNAs enriched with AGA and GAA codons under both normal and stress conditions. In this report, we studied the role of *alkb-8* in *C. elegans*. We show that downregulation of *alkb-8* increases detection of lysosome-related organelles visualized by Nile red *in vivo*. Reversely, forced expression of *alkb-8* strongly decreases the detection of this compartment. In addition, overexpression of *alkb-8* applied in a pulse during the L1 larval stage increases *C. elegans* life span.

Introduction

The 2OG/Fe(II) (2-oxoglutarate- and Fe^{2+}-dependent) oxygenase superfamily possess an important position in-between oxygenases. The heme group is substituted in these enzymes by a protein module that coordinates Fe^{2+} and whose enzymatic activity is dependent on 2-oxoglutarate that serves as an electron donor and is consumed during the enzymatic reaction while converted to succinate and carbon dioxide. Unlike monooxygenases that are dependent on heme and which transfer one oxygen atom to

65 the substrate and reduce the other oxygen atom to water, 2OG/Fe(II) oxygenases
66 incorporate both atoms of molecular oxygen (O_2) into the product(s) of the reaction and
67 are classified as dioxygenases. 2-oxoglutarate is a rate-limiting factor for enzyme
68 catalytic activity for its critical intracellular concentration level. Enzymes of this
69 category function in a wide spectrum of metabolic processes including posttranslational
70 modification of proteins, DNA repair, epigenetic modification of DNA and the
71 regulation of hypoxia responsive genes (Aravind & Koonin 2001; van den Born et al.
72 2011; Fedeles et al. 2015).
73 The AlkB family of dioxygenases encompasses homologues of AlkB from
74 *Escherichia coli* which is a DNA repair enzyme demethylating methylated DNA and
75 RNA bases (e.g. 1-methyladenine and 3-methylcytosine). Mammalian AlkB
76 homologues include 9 genes, named ALKBH1 to 8 and a fat mass and obesity
77 associated protein FTO originally identified as a gene localized at a chromosomal locus
78 associated with the rat fussed-toes phenotype (Peters et al. 1999; Gerken et al. 2007;
79 Fedeles et al. 2015). FTO gene received attention for its association with human obesity
80 (Frayling et al. 2007; Yajnik et al. 2009) later in part shown to be associated with a
81 homeobox gene IRX3 that is regulated by noncoding sequences within the *FTO* gene
82 (Smemo et al. 2014). This connection is conserved between fish and mammals. Besides
83 that, FTO has its own role in obesity as its global overexpression lead to hyperfagia and
84 obesity (Church et al. 2010).
85 ALKBH8 homologues have a special position among all AlkB proteins for possessing
86 two extra domains in addition to the dioxygenase domain, a methyl transferase domain
87 and an N-terminal RNA recognition motif that likely helps the AlkB domain in search
88 for specifically modified tRNAs (Songe-Moller et al. 2010; Pastore et al. 2012).
89 ALKBH8 has been shown to regulate the rate of protein synthesis from mRNAs that are

coded by codons for which there is a limited amount of tRNA through the modification of bases in the anti-codon region of tRNA especially the wobble base, the first base in the anti-codon place of tRNAs, that can following this modification recognize additional codons (Songe-Moller et al. 2010; van den Born et al. 2011). ALKBH8 was shown to have a role in urothelial carcinoma cell survival mediated by NOX-1-dependent ROS signals. Silencing of ALKBH8 induced JNK/p38/gammaH2AX-mediated cell death (Shimada et al. 2009). The role of human ALKBH8 as a tRNA methyltransferase required for wobble uridine modification and DNA damage survival is well documented. Fu at al. showed that the AlkB domain of mammalian ALKBH8 catalyzes hydroxylation of 5-methoxycarbonylmethyluridine at the wobble position of tRNA (Fu et al. 2010a; Fu et al. 2010b). The AlkB domain of ALKBH8 specifically hydroxylates mcm(5)U into (S)-mchm(5)U diastereomer in tRNA-Gly(UCC) (van den Born et al. 2011).

The ALKBH8 methyltransferase domain shows close relationship to a yeast methyltransferase TRM9. The function of the yeast TRM9 has been investigated (Kalhor & Clarke 2003; Deng et al. 2015). The enzyme catalyses the methylation of the wobble bases at position 34 in tRNA. U at this position can recognize all four bases while the modified uridine residues are more restrictive and limit the recognition to only A and G, or to only one of these residues. Codon-biased translation can be regulated by wobble base tRNA modification systems during cellular stress responses (Chan et al. 2010; Chan et al. 2012; Gu et al. 2014). This mechanism is conserved in plants. In *Arabidopsis thaliana* the Trm9 orthologue (AtTRM9, AT1G31600) and two other ALKBH8-like proteins AtTRM112a and AtTRM112b function in the formation of modified wobble uridines. AtTRM9 is responsible for the final step in mcm(5)U formation. The enzymatic activity of AtTRM9 depends on either AtTRM112a or

AtTRM112b. *A. thaliana* ALKBH8 orthologue AtALKBH8 is required for hydroxylation of mcm(5)U to (S)-mchm(5)U in tRNA(Gly)(UCC). Plants with mutant atalkbh8 have increased levels of mcm(5)U and of mcm(5)Um, its 2'-O-ribose methylated derivative, suggesting that accumulated mcm(5)U is prone to further ribose methylation by another mechanism (Leihne et al. 2011). Protozoan ALKBH8 oxygenases display both DNA repair and tRNA modification activities (Zdzalik et al. 2014).

ALKBH8 was shown to regulate selenocysteine-protein expression as a protective mechanism against damage by reactive oxygen species (Endres et al. 2015). *C. elegans* has two thioredoxin reductases, TRXR-1 and TRXR-2 (Buettner et al. 1999) but only one of them, TRXR-1 is a selenoprotein. Thioredoxin (TRX-1) is related to life span regulation and oxidative stress response in *Caenorhabditis elegans* (Jee et al. 2005; Miranda-Vizuete et al. 2006). TRXR-1 and TRXR-2 have differential physiological roles in *C. elegans* and localizations. TRXR-1 is a cytosolic protein. TRXR-2 is mitochondrial and protects mitochondria from oxidative stress, where reactive oxidative species are mainly generated, while cytosolic TrxR plays a role to maintain optimal oxido-reductive status in the cytosol. The cytosolic *trxr-1* is highly expressed in pharynx, vulva and intestine. *trxr-2* is mainly expressed in pharyngeal and body wall muscles and its defects cause a shortened life span and a delay in development under stress conditions. Deletion mutation of the selenoprotein *trxr-1* results in decreased acidification of the lysosomal compartment in the intestine. Interestingly, the acidification defect of *trxr-1*(jh143) deletion mutant was rescued, not only by selenocystein-containing wild type TRXR-1, but also by a cysteine-substituted mutant TRXR-1. Both *trxr-1* and *trxr-2* were up-regulated when worms were challenged by environmental stress such as heat shock (Li et al. 2012).

A prominent feature of *C. elegans* enterocytes are lysosome-related organelles (LRO) called gut granules. Similarly as mature lysosomes, gut granules have internal acidic pH, contain hydrolytic enzymes and lack mannose-6-phosphate receptors. Gut granules are highly heterogeneous when analyzed by electron microscopy, display various level of birefringence in light microscopy and autoflorescence, which increases with animal age. In *C. elegans*, staining by Nile red applied on animals *in vivo* together with bacterial food allows highly reproducible functional determination of a specific subpopulation of lysosome-related organelles (Soukas et al. 2013). *In vivo* Nile red uptake may be used as an effective tool for identification of proteins that function at the level of specific LRO (Soukas et al. 2013).

In this report, we attempted to functionally characterize ALKB-8 in *C. elegans*. We show that *alkb-8* downregulation by RNAi leads to slightly accelerated larval development and elevated values of *in vivo* Nile red compartment staining. The forced expression of *alkb-8* downregulates this subcellular compartment. While downregulation of *alkb-8* does not affect *C. elegans* longevity, forced expression of *aklb-8* increases *C. elegans* life span by approximately 30%.

Materials and Methods

Maintenance of *C. elegans* strains and transgenic lines

All *C. elegans* strains were maintained as described (Brenner 1974). The wild type strain N2 (var. Bristol) was obtained from the *C. elegans* Stock Center (https://cgc.umn.edu/).

Transgenic lines were prepared by microinjections of plasmid DNA into gonads of young adult N2 hermaphrodites using an Olympus IX70 microscope equipped with Narishige microinjection system (Olympus, Tokyo, Japan). Injections were done as described (Fire et al. 1998; Tabara et al. 1999).

Synchronized populations of L1 larvae were prepared by the „Bleaching“ technique where the cultured nematodes are treated with alkaline hypochlorite solution, which destroys all larval stages except the embryos that are protected by egg shells. Embryos hatch in liquid solution without access to food, which prevents further development. The protocol is described in (Porta-de-la-Riva et al. 2012).

Isolation of genomic DNA

The genomic DNA used as a template for PCR reactions was isolated using High Pure PCR Template Preparation Kit (Roche Diagnostics, Mannheim, Germany). For isolation we used about 50 mg of washed wild-type animals of mixed developmental stages and we followed the manufacturer´s protocol “Isolation of Nucleic Acids from Mammalian Tissue”.

Total RNA isolation and cDNA synthesis

Total RNA was isolated from N2 animals kept on 2% agarose plates. Animals of the required developmental stage and feeding status were washed with water, pelleted by centrifugation for 5 min at 200 x g and frozen at -80 °C. The frozen pellet was quickly melted and resuspended in 0,5 ml of resuspension buffer (0,5% SDS; 5% 2-

mercaptoethanol; 10 mM EDTA; 10 mM Tris/HCl (pH 7,5) with 12,5 µl of proteinase K (20 mg/ml)), vortexed for 1 min and incubated 60 min at 55 °C. RNA was isolated by phenol-chloroform extraction and ethanol precipitation and the pellet was dissolved in water. The sample was then treated with 1 unit of DNase I (New England Biolabs, Ipswich, MA) per 1µg of total RNA for 30 min at 37 °C and purified by phenol-chloroform extraction and ethanol precipitation followed by RNA resuspention in DEPC water.

Complementary DNA (cDNA) was prepared with SuperScript III First-Strand Synthesis System for RT-PCR (Invitrogen, Carlsbad, CA, USA) with random hexamers, according to manufacturer's protocol.

Quantitative PCR

Total RNA from individual developmental stages (embryos, L1, L2, L3, L4 and young adult animals) and from fasted and fed animals was isolated and used for cDNA synthesis as described above. Quantitative PCR (qPCR) was performed using the Universal Probe Library technique (Roche Molecular Systems, Inc. Pleasanton, CA, USA). Primers and probes were designed with Universal Probe Library System Assay Design Software. Reactions were run on LightCycler 2.0 with the software LightCycler 4.1 (Roche Molecular Systems, Inc. Pleasanton, CA, USA) and the protocol described earlier (Vohanka et al. 2010) was used. The expression was normalized against *ama-1*. All samples were run in triplicates. The expression ratio (ΔΔCt) is calculated using the efficiency corrected model. In different developmental stages the resulting values mean fold change of expression compared to expression in embryos. In fasting experiments the result is fold change of expression compared to fed control animals.

208

209 **RNA interference**

210 For downregulation of *alkb-8* expression we used the RNAi feeding method
211 where animals are fed on bactria producing dsRNA as previously described (Timmons
212 et al. 2001).
213 For preparation of the feeding vector we first cloned the whole cDNA sequence of *alkb-*
214 *8* into pCR®II vector using TA Cloning® Kit Dual Promoter (pCR®II) (Invitrogen,
215 Carlsbad, CA, USA). Primers used for the PCR reaction were 11/08 (5´
216 ATGTATTTCAATGAAGAAAAAGCGA 3´) and 10/08 (5´
217 TCAAATTTTCTTCGCAATAATAATATAA 3´). Then the *alkb-8* sequence was
218 recloned into the L4440 vector using enzymes Hind III and Xba I. The *E. coli* strain
219 HT115 was transformed with *alkb-8*::L4440 and empty L4440 control vector and one
220 colony from each was inoculated to LB medium with Ampicillin (100 μg/ml final
221 concentration) and let grown to $OD_{600} \approx 0,4$. Then isopropyl β-D-1-
222 thiogalactopyranoside (IPTG) was added to culture to a final concentration of 0,4 mM
223 to induce dsRNA production. The culture was grown for 4 hours at 37 °C and then 300
224 μl was plated onto NGM plates supplemented with Ampicillin (100 μg/ml final
225 concentration) and IPTG (0,4 mM final concentration). The plates were kept at room
226 temperature overnight and the next day synchronized L1 larvae were placed on these
227 plates.

228 **Nile red staining**

229 For the estimation of LRO compartment visualization by *in vivo* Nile red uptake
230 and resulting fluorescence, the synchronized L1 larvae (control larvae, larvae inhibited
231 for *alkb-8* by RNAi or larvae with forced overexpression of *alkb-8*) were transferred on

feeding culture + 50 ng Nile red / ml of culture. 300 µl of OP50 culture with Nile red was used per plate. Nematodes were kept at 22 °C for 48 h and then fluorescent pictures of young adults were acquired using identical settings and exposure times (magnification with 20x objective, exposure time 10 ms in RNAi experiments and 50ms in overexpression experiments). Resulting images were analyzed using the ImageJ program (https://imagej.net/). The total pixel intensity of the cytoplasmic area of the first two intestinal cells in images yielding highest fluorescence was determined and used for comparison.

Overexpression of *alkb-8*

The entire cDNA sequence of *alkb-8* was recloned from pCRII vector into the expression vectors which contain heat shock inducible promoter pPD49.78 and pPD49.83 using restriction enzymes EcoRV and KpnI. Constructs were injected into N2 hermaphrodites (at a concentration of 50ng/µl) along with a positive selection marker, pRF4 plasmid (50 ng/µl), which encodes a mutant collagen *(rol-6*(su1006)) that induces a dominant "roller" phenotype. As control we used animals injected only with pRF4 plasmid.

Forced expression was induced in a synchronized population of L1 animals. Larvae were placed on plates seeded with OP50 bacterial culture and were left for 2 hours at RT for recovery and then subjected to 30 min heat shock at 34 °C, after which the animals were kept at 22°C and life span was determined. In case of Nile red staining experiment, the bacterial culture was supplemented with 15 ng of Nile red per plate. Pictures were taken after 50 hours using a constant setting.

Preparation of *alkb-8*::*gfp* transgene regulated by CEOP3136 promoter and endogenous 3' UTR

According to WormBase (WS263) *alkb-8* is organized in a hybrid operon CEOP3136. This operon includes four genes, *wdr-5*, *dph-1*, *alkb-8* and *nrde-1*. Since the expression from a transgene regulated by the internal *alkb-8* promoter is already known, we constructed an expression vector to prepare transgene expressing ALKB-8 tagged with GFP under the regulation of operon promoter and *alkb-8* endogenous 3' UTR. To achieve this, four amplified DNA fragments containing the operon promoter, *alkb-8* genomic sequence, gene coding for GFP and the 3'UTR of *alkb-8* were amplified (primer sequences are listed in Table 1) and assembled using GENEART® Seamless Cloning and Assembly Kit (Invitrogen, Carlsbad, CA, USA) according to the manufacture´s protocol. The resulting product was verified by sequencing and used for preparation of transgenic lines (injected in a concentration of 50 ng/µl without pRF4 vector). The scheme of the construct is shown in **Fig. 1.**

Table 1. Primers used for seamless cloning and assembly of the $P_{CEOP3136}$::*alkb-8::gfp*::*alkb-*$8_{3'UTR}$ construct.

Primer	sequence 5´→ 3´		Note
11/80	AATTCGAGCTCGGTACGGATAAGGAAGATCATCAATGTTT	S	CEOP3136 promoter
11/81	TCACACATATCTGAAATCACAGCAAAAATCAA	AS	CEOP3136 promoter

11/82	TTTCAGATATGTGTGAGTTCATTTTTCAACCC	S	*alkb-8* gDNA
11/83	GGGTCCTCAATTTTCTTCGCAATAATAATATA	AS	*alkb-8* gDNA
11/84	AGAAAATTGAGGACCCTTGGAGGGTACCGGTA	S	*gfp*
11/85	TAAAAAAACTATTTGTATAGTTCATCCATGCC	AS	*gfp*
11/86	ACAAATAGTTTTTTTAAAGTTTTTTCTATTGG	S	*alkb-8* 3'UTR
11/87	GCCAAGCTTGCATGCCTTTAGCGCAGTTTGAGAATCTGAA	AS	*alkb-8* 3'UTR

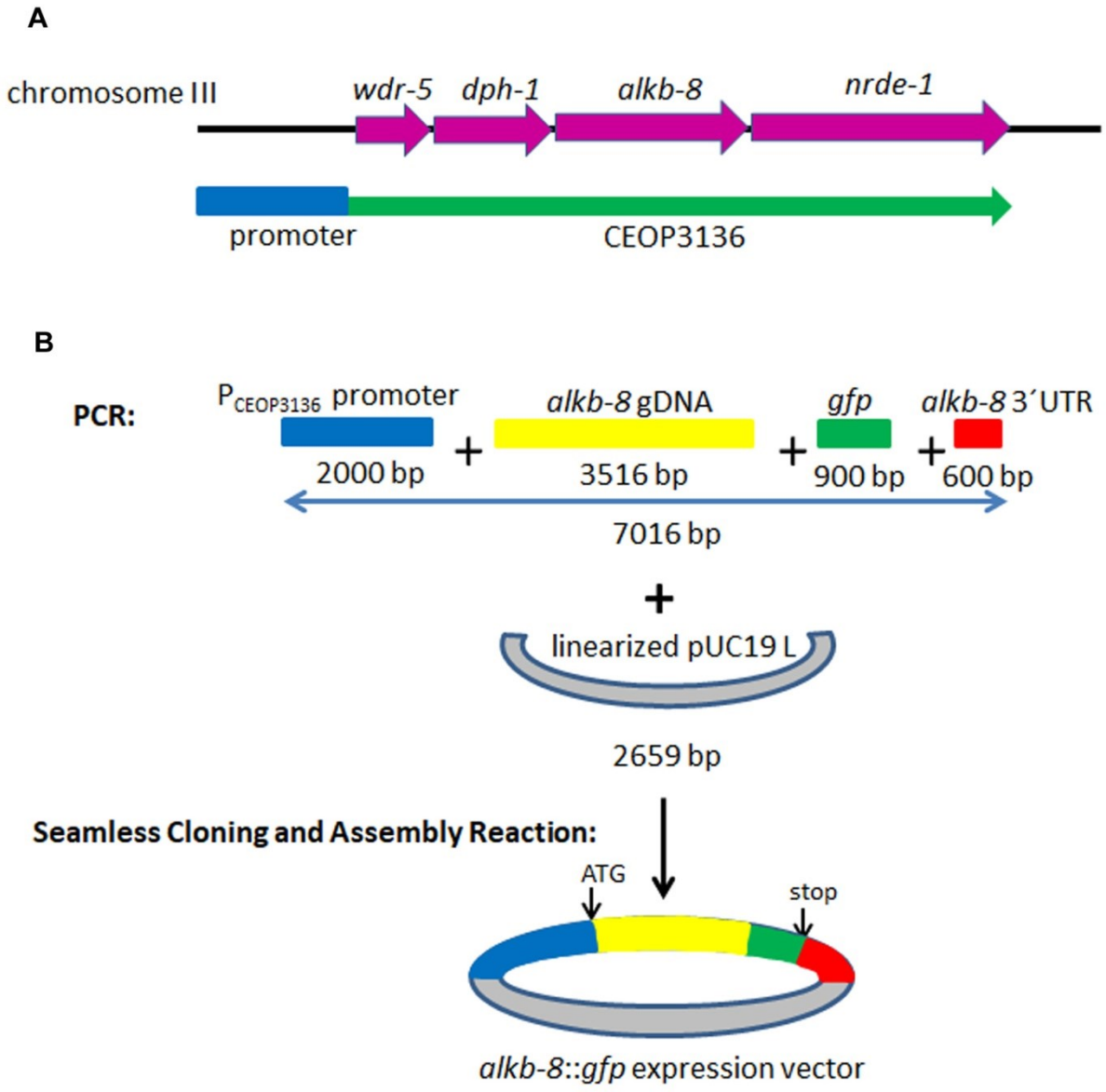

Fig. 1 Preparation of the transgenic line expressing *alkb-8::gfp* under the regulation of promoter of CEOP3136 and endogenous 3' UTR. A – Organization of *alkb-8* on chromosome III. *alkb-8* is the third gene in operon CEOP3136 and has its own internal promoter. B – Strategy for preparation of transgene expressing ALKB-8 tagged by GFP at its 3' end. Corresponding fragments of CEOP3136 promoter, *alkb-8* genomic sequence, gene coding for GFP based on pPD95.75 and *alkb-8* 3'UTR were amplified by PCR and assembled by Seamless Cloning Assembly Reaction.

Developmental assay

To estimate the timing of larval development of control *C. elegans* and animals with *alkb-8* downregulated by RNAi, the synchronized population of L1 larvae was prepared and equal volumes of liquid larval culture were transferred to control plates containing HT115 bacteria with empty L4440 plasmid and plates containing bacteria transfected with the same plasmid but containing the cloned insert of *alkb-8*. Both bacterial cultures were induced by IPTG. The experiment was done in quadruplicate from which one representative set was selected for more specific analysis. Equal surface of plates with experimental (photographed first) and control animals was photographed at the time when control animals started to first lay eggs (after 78 hours at 16 °C) and the number of animals and laid eggs was determined on the photographs. The pictures were taken on Olympus SD30 microscope (Olympus, Tokyo, Japan) with Panasonic DMC-TZ3 camera (Panasonic, Kadoma, Japan).

Life span determination

For determination of life span, a large scale of synchronized N2 L1 larvae was prepared and divided to control cultures and cultures subjected to *alkb-8* dsRNA produced by bacteria that were fed to experimental animals and synchronized populations of transgenes containing *rol-6* gene as control and experimental animals carrying extrachromosomal arrays containing *rol-6* and *alkb-8* cloned in heat shock vectors pPD49.83 and pPD49.78. For each experimental condition, 100 L1 larvae were selected and followed on a daily basis throughout their complete life span in the overexpression experiment. In RNAi experiments 60 animals were followed in each group.

Microscopy

Nomarski optics microscopy and fluorescence microscopy pictures were taken with Olympus BX60 microscope equipped with DP30BW CD camera (Olympus, Tokyo, Japan). Confocal microscopy was done using an inverted Leica SP8 TCS SMD FLIM system equipped with a 63 × 1.2 NA water immersion objective, a pulsed white light laser (470-670 nm), AOBS and two internal hybrid single photon counting detectors, and operated by Leica Application Suite X program (Leica Micosystems, Wetzlar, Germany).

Results

Expression of *alkb-8* continues from embryonic stages through larval development to adults

We analyzed the gross expression of *alkb-8* during developmental stages using reverse transcription-quantitative PCR. The results were normalized for the expression of Polymerase II subunit *ama-1* and related to the expression observed in mixed stages embryos. The relatively high expression of *alkb-8* in embryos decreased in synchronized L1 larvae and steadily increased from L2 stage to young adults (Fig. 2a). We analyzed the effect of 6 hours fasting and feeding in synchronized L1 larvae on the level of expression of *alkb-8* (and *fat-7* and *asc-2*, for which the response to starvation is known). Starvation had no effect on *alkb-8* expression while *fat-7* and *asc-2* expression responded to fasting as expected.

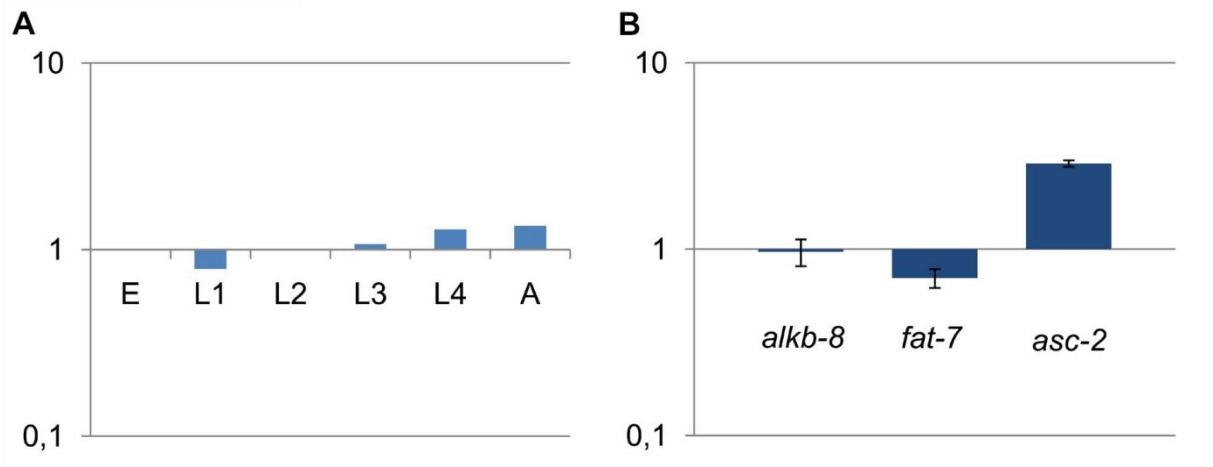

Fig. 2 The expression profile of alkb-8 gene analyzed by RT-qPCR. A-The expression of *alkb-8* during development. Results are shown in logarithmic scale and the values represent fold change of expression compared to expression in embryos. The expression drops in the L1 stage and gradually increases during development. B- The relative expression of *alkb-8* after six hours of fasting. The values represent fold change

of expression compared to fed control animals. The expression of *alkb-8* is not affected by the feeding status. Genes previously reported to be affected by fasting (Van Gilst et al. 2005), *fat-7* (expression decreases after fasting) and *asc-2* (increases) were used for control.

Tissue- and cell-specific expression of *alkb-8* from the operon promoter

According to WormBase (WS263) *alkb-8* is organized as a third gene in a hybrid operon CEOP3136 indicating that its expression depends partially on the operon promoter and partially on its own promoter. Expression of *alkb-8* dependent on the internal promoter was described by Pastore and coworkers and revealed *alkb-8* expression decreasing during later larval stages and the expression pattern was restricted to a small number of cells, especially several neurons (Pastore et al. 2012). For visualization of *alkb-8* expression dependent on the operon promoter, we prepared lines carrying extrachromosomal arrays containing the transgene consisting of the CEOP3136 promoter, *alkb-8* genomic sequence fused to *gfp* and followed by the endogenous *alkb-8* 3'-UTR. The transgene is expressed ubiquitously in embryos from approximately the 40 cell stage throughout the embryonic development. The expression continued in L1 larvae, although it was necessary to use longer time exposure for its visualization in accordance with the decreased expression observed in L1 larvae in the RT-qPCR experiment. The cytoplasmic expression of the transgene was strong in neurons, pharyngeal and body wall muscles, and other tissues such as somatic gonad and the egg-laying apparatus (**Fig.3** and **Fig. 4**). We also observed diffuse expression in intestinal cells (**Fig. 3**).

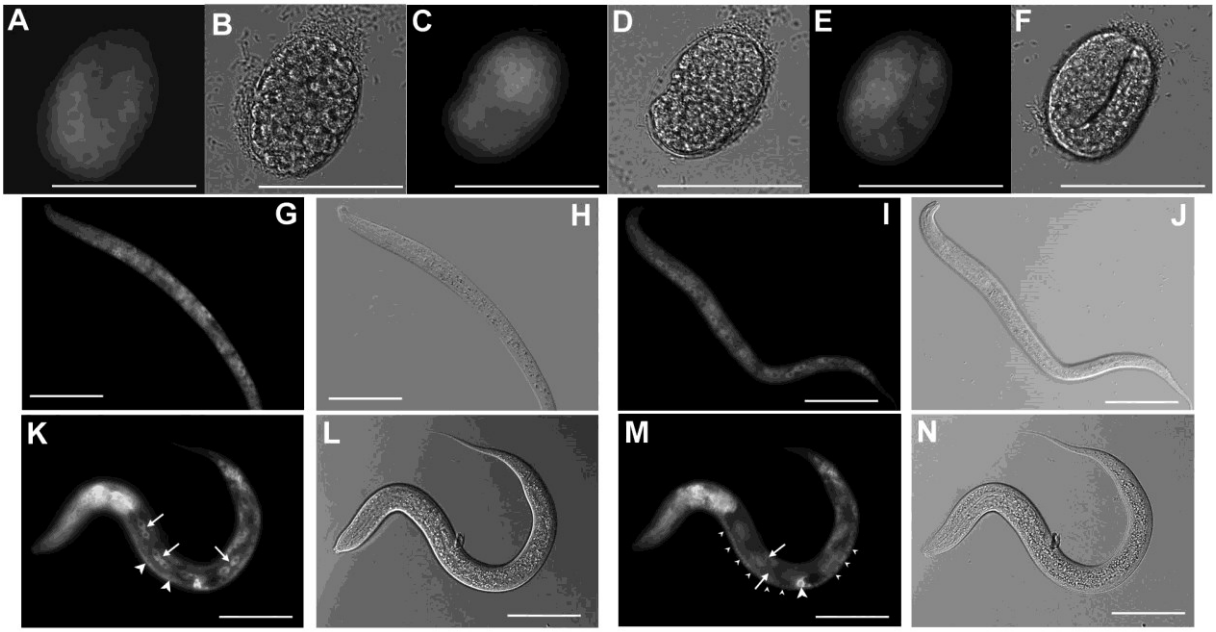

Fig. 3 Expression pattern of ALKB-8::GFP in early stages of development using a transgenic line carrying an extrachromosomal DNA construct.

The construct composition is shown in Fig. 1. The GFP signal in embryos can be detected early after eggs are laid (around 40 cells stage) shown in panels A and B. The expression continues to be ubiquitous during embryonic development; panels C and D show an embryo at the end of the gastrulation phase, panels E and F an embryo at the 2-fold stage. Panels G to J show early L1 larvae where the GFP signal is detected in all cell types with similar intensity. In the L1/L2 developmental stage (panels K through N) the expression starts to be differentiated and the highest signal is seen in pharyngeal and neuronal cells in the head and tail areas. Strong signal is also detected in seam (arrows) and muscle cells (arrowheads) in panel K. In panels M and N the same animal as shown in panels K and L but with focus on a different layer. High expression is visible in intestinal cells (arrows), the distal tip cell (DTC) (arrowhead) and in the ventral nerve

cord (small arrowheads). Pictures in panels A, C, E, G, I, K and M are taken in GFP fluorescence and panels B, D, F, H, J, L, N in Nomarski optics. Bar represent 50 µm.

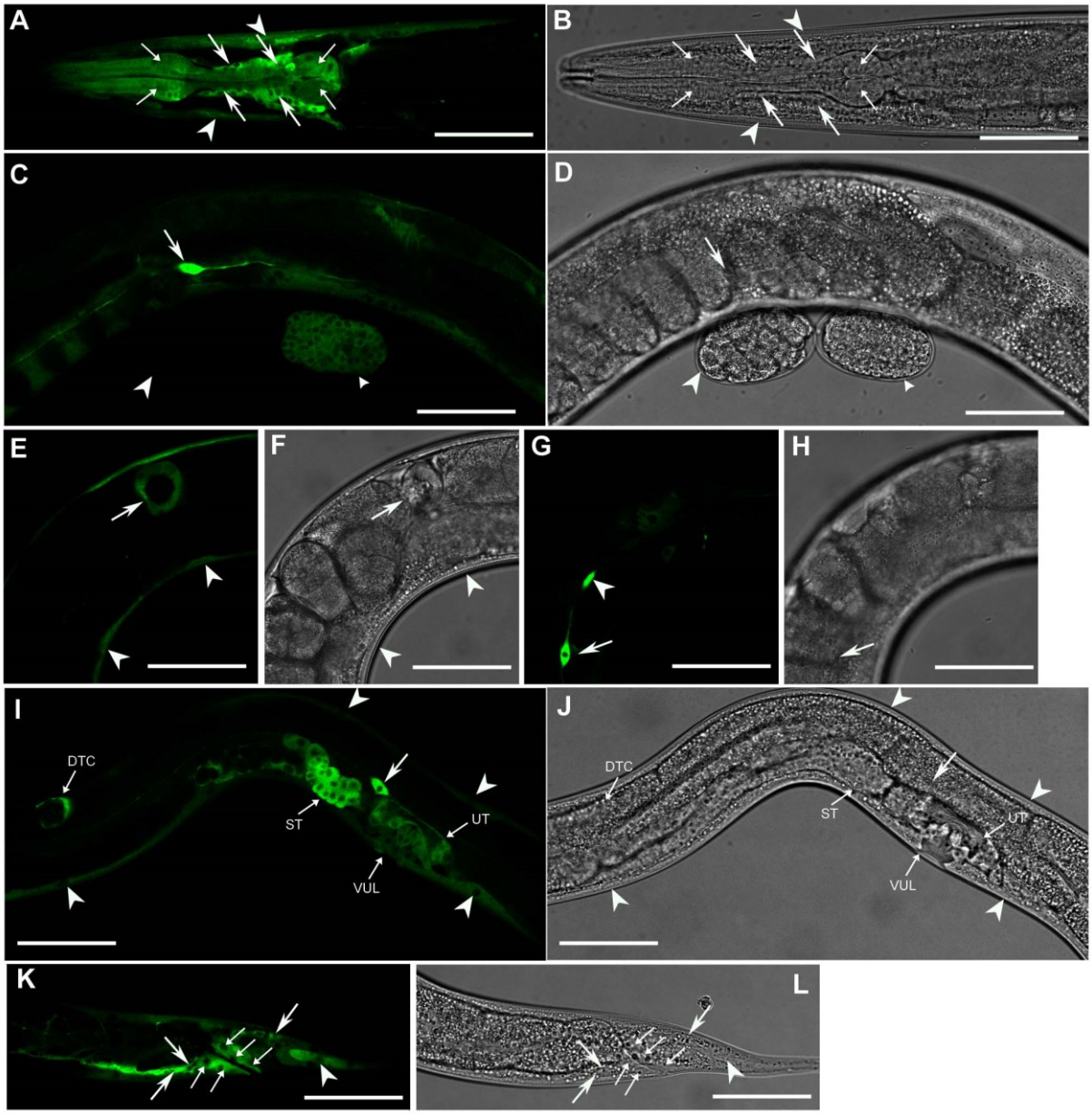

Fig. 4 Expression of *alkb-8::gfp* from extrachromosomal arrays regulated by the promoter of CEOP3136 operon analyzed by confocal microscopy. Panel A shows the expression of *alkb-8::gfp* in the head of an adult animal. Strong signal is detected in

neurons (arrows), pharyngeal muscle cells (small arrows) and head muscle cells (arrowheads). Panel B – shows the same animal as panel A but in Nomarski optics. Panels C and D show the central part of the body of an adult animal with two freshly laid embryos. The embryo in the left is approximately in the 30 cells stage (arrowhead) and shows no expression of *alkb-8::gfp.* In contrast, the embryo on the right is in the approximately 100 cells stage (small arrowhead) and shows ubiquitous cytoplasmic expression of the transgene. The canal-associated neuron (CAN) marked by arrow shows strong cytoplasmic expression of the transgene. Panels E and F show expression of *alkb-8* in the spermatheca (arrow) and body wall muscles (arrowheads). Panels G and H show another focal plane of the same animal as showed in E and F. The arrow indicates strong expression in the CAN neuron and in another unidentified neuron (arrowhead). Panels I and J show the central part of the body of a L4 larva where high expression of *alkb-8* is detected in cells of the somatic gonad and egg-laying apparatus indicated by small arrows (DTC- distal tip cell, ST- spermatheca, UT- uterus, VUL- vulva). Large arrow points to the CAN neuron, arrowheads point to body wall muscles. Panels K and L show the distant part of a L4 larva with many *alkb-8* positive cells. Tail neurons (arrows), hyp cell (arrowhead) and rectal epithelial cells (small arrows) are indicated. Panels B, D, F, H, J and L shows the same picture as the fluorescent picture on their left in Nomarski optics. Bars represent 50 μm.

The effects of *alkb-8* downregulation and forced overexpression on *C. elegans* development

Downregulation of *alkb-8* by RNAi using the protocol with bacteria producing dsRNA did not reveal any directly observable phenotype. In contrary, the larvae with

downregulated *alkb-8* seemed to be in a very good feeding status and possibly slightly bigger than the controls fed with bacteria containing empty vector expressing short non-specific dsRNA. Since the observed difference was not causing delays in complete larval stages, we analyzed the onset of egg laying in control and RNAi treated cultures. This strategy revealed clearly observable difference in time given by the onset of egg laying by control larvae at which the larvae with downregulated *alkb-8* laid already approximately 50 times more embryos (Fig. 5). No specific developmental defects were observed.

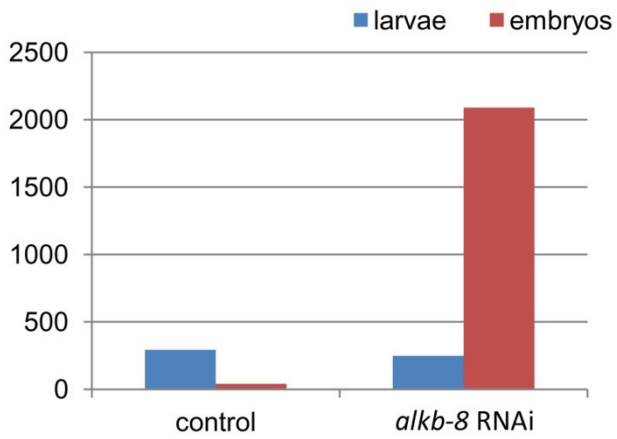

Fig. 5 Analysis of the effect of alkb-8 downregulation by RNAi on *C. elegans* larval development. Equal amounts of synchronized L1 larvae were transferred on plates with control cultures (HT115 bacteria transformed with empty L4440 vector) and experimental plates seeded with bacteria transformed with L4440 vector containing *alkb-8* cDNA. Both control and experimental plates were induced using IPTG and the cultures observed to the time point when control animals start to lay eggs. At this time, equal areas of plates with nematodes were photographed and the number of animals (and laid eggs) was determined. The experiment shows that inhibition of *alkb-8* by the

feeding method that was used in this experiment doesn't affect the larval development of *C. elegans*. In contrary, animals with downregulated *alkb-8* developed faster compared to control animals**.**

The effect of *alkb-8* downregulation and forced overexpression on the visualization of the Nile red-positive compartment

In order to assess a possible involvement of ALKB-8 in the function of lysosome-related organelles, we assayed the uptake of Nile red delivered to nematode synchronized cultures together with bacterial food. Animals with inhibited *alkb-8* showed markedly higher Nile red dependent fluorescence in enterocytes. In both experimental and control animals, the Nile red fluorescence was higher in proximal enterocytes compared to enterocytes of the middle part of the gut. We therefore analyzed the fluorescent signal in the first two proximal enterocytes. Densitometric analysis of Nile red-dependent fluorescence confirmed an approximately 30% increase of the Nile red positive signal in animals with inhibited *alkb-8* (Fig. 6).

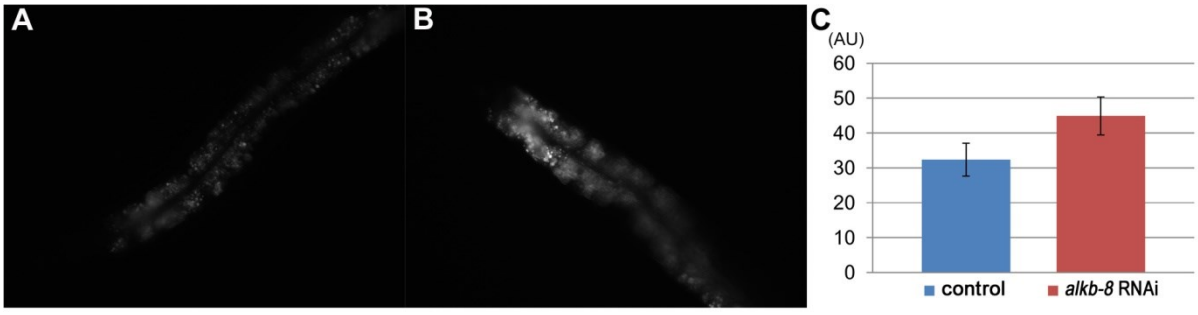

Fig. 6 Detection of the signal in the *in vivo* Nile red stained compartment in control animals and animals with downregulated *alkb-8*. Panel A shows a Nile red derived fluorescence in a young adult control animal. Panel B shows a larva with *alkb-8* inhibited by RNAi with the identical optical settings. Panel C shows the result of densitometric analysis of Nile red derived fluorescence in the two most proximal enterocytes of 23 animals with downregulated *alkb-8* and 21 control animals. The results show a pronounced increase of approximately 30 % of Nile red derived fluorescence in animals with *alkb-8* down regulated by RNAi compared to control animals. $P < 0{,}001$.

We also assayed if forced expression of *alkb-8* affects the Nile red positive fluorescence in enterocytes. Two transgenic lines expressing *alkb-8* from extrachromosomal arrays under the regulation of heat shock regulated promoter based on the plasmid pPD49.78 and pPD49.83 were prepared. Both plasmids lead to the transgene expression in a wide spectrum of cells and differ in the extent of the expression in intestinal cells, which is higher in case of pPD49.83. Both transgenic lines showed a strong decrease in the extent of Nile red positive signal in enterocytes (Fig. 7). Keeping with ALKB-8 intestinal role, the line based on pPD49.83 which leads to a strong intestinal expression of the transgene showed the lowest values for Nile red dependent fluorescence.

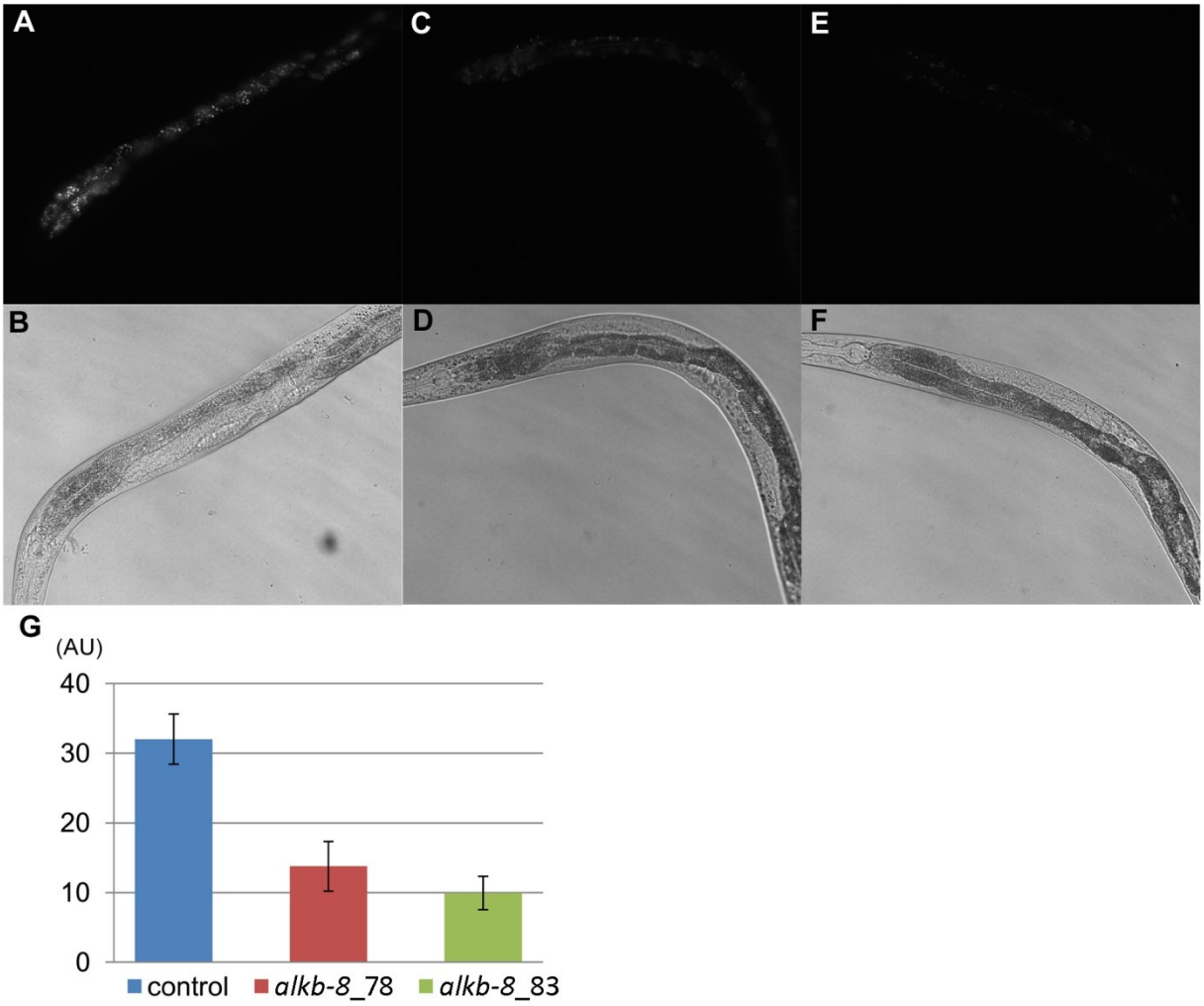

463

464 **Fig. 7 The effect of *alkb-8* forced overexpression on the signal of the Nile red**
465 **positive compartment of LRO.** Panels A, C and E show fluorescence images of young
466 adult larvae stained in vivo with Nile red. Panel A- shows an animal from the control
467 group, panel C- an animal from the group overexpressing *alkb-8* from pPD49.78 vector,
468 panel E- an animal from the group with *alkb-8* in pPD49.83 vector. Panels B, D and F
469 show the same pictures as the pictures next to them in Nomarski optics. Panel G shows
470 the result of Nile red staining analysis after forced expression of *alkb-8* calculated just
471 as in the RNAi experiment. Overexpression of *alkb-8* from pPD49.78 decreases Nile
472 red staining in intestinal cells by 60 % (marked as *alkb-8*_78) and from pPD49.83
473 (marked as *alkb-8*_83) by 70 % compared to control animals. $P < 0{,}0001$

474

475 **The effect of *alkb-8* overexpression on *C. elegans* life span**

476 To determine if the effect of ALKB-8 on the Nile red positive compartment has a
477 broader metabolic role, we assayed the life span of animals with downregulated *alkb-8*
478 expression or pulse-overexpressed *alkb-8.* Downregulation of *alkb-8* expression
479 (applied for the entire lifetime of the assayed animals) had no effect on the animal life
480 span (Fig. 8). In strong contrast, pulse forced expression in animals during their L1
481 stage led to pronounced life span extension of experimental animals reaching 10 to
482 40%.

483

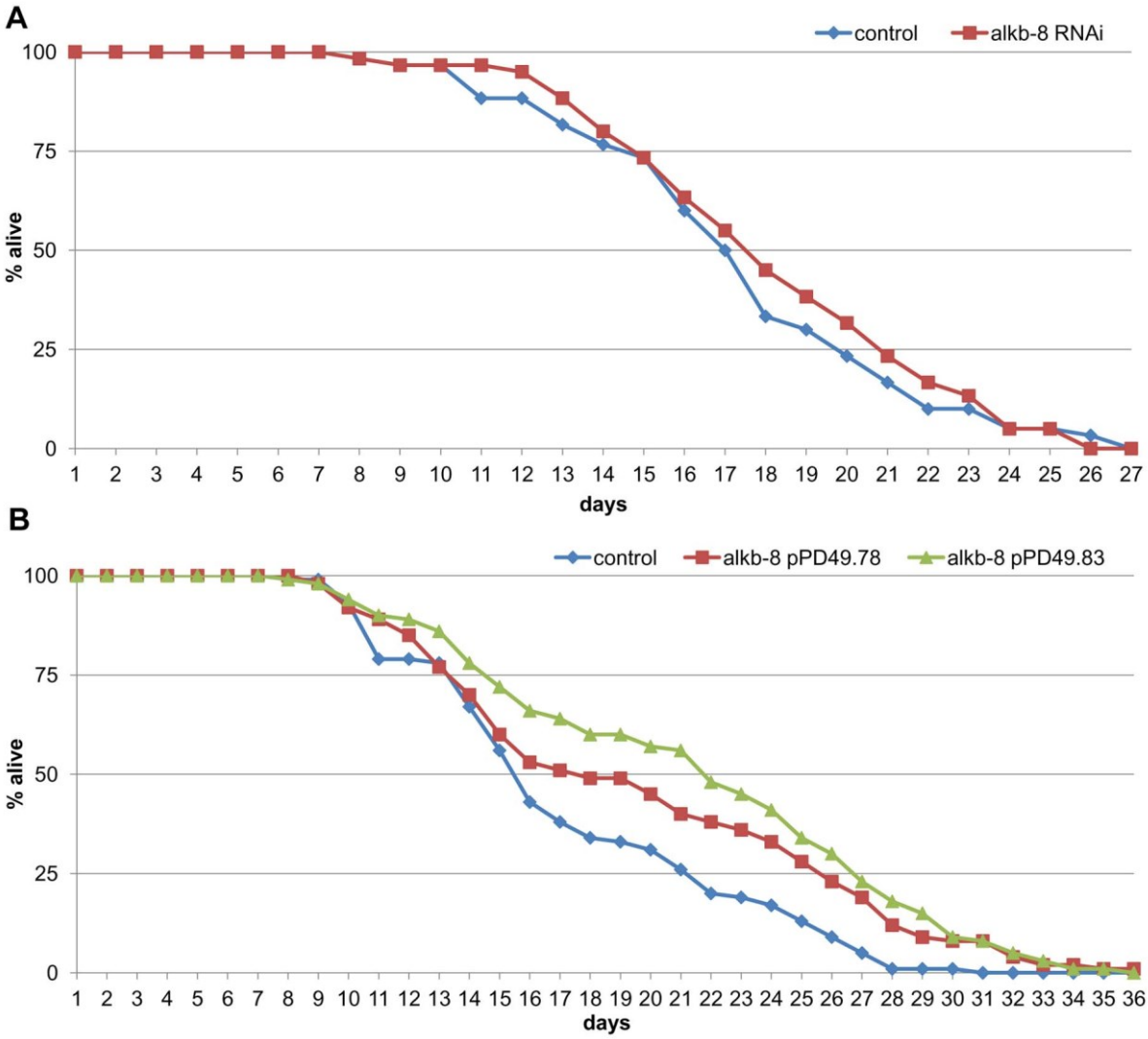

Fig. 8 Determination of the effect of *alkb-8* on the life span of *C. elegans*. Panel A – The effect of *alkb-8* downregulation on nematode longevity. Animals inhibited for *alkb-8* to the level that is affecting Nile red positive compartment staining has no effect on nematode longevity. Panel B – the effect of pulse overexpression in L1 stage on *C. elegans* longevity. Compared to controls, animals with forced expression of *alkb-8* have life span extended by 10 to 40 %.

Discussion

Our results support ALKB-8 modulatory function in metabolic events linked to lysosome-related organelles and aging in *C. elegans*. Surprisingly, despite that *alkb-8*

494 being expressed strongly and ubiquitously from early embryonic stages to adulthood, its
495 downregulation by RNAi to levels that affect the detection of lysosome-related
496 organelles by *in vivo* Nile red staining do not harm embryonic development. This
497 suggests that the sensitivity of lysosome-related organelles to ALKB-8 levels is greater
498 than a possible involvement in developmental events. Keeping with the metabolic roles
499 of ALKB-8, its overexpression applied during the first larval stage markedly prolonged
500 life span. On the other hand, downregulation of *alkb-8* by RNAi does not shorten their
501 life span. There are several factors that may cause this discrepancy. Firstly, RNAi is not
502 significantly affecting neuronal cells in wild type N2 *C. elegans* unless specific lines are
503 used for silencing experiments (Simmer et al. 2002) and thus a proportion of ALKB-8
504 responsible for the observed phenotypes may be unaffected in *alkb-8* downregulation
505 experiments. The experiments with *alkb-8* forced overexpression are likely to lead to
506 elevated levels of ALKB-8 in most cells, except in the gonads. It can be assumed that
507 the effects on the extent of detection of the *in vivo* Nile red positive compartment is at
508 least partially a result of ALKB-8 direct function in enterocytes. The effect on longevity
509 may be to a large extent based on neuronal functions of ALKB-8. In agreement with
510 this, in *rrf-3* mutant animals, in which RNAi affects also neuronal cells, neuronal
511 inhibition of the autophagy nucleation complex extends life span of *C. elegans*. The
512 authors demonstrated that inhibition of the VPS-34/BEC-1/EPG-8 autophagic
513 nucleation complex as well as its upstream regulators strongly extend *C. elegans* life
514 span and that post-reproductive inhibition of *bec-1* mediates longevity specifically
515 through the neurons (Wilhelm et al. 2017).

516 The positive effect of ALKB-8 on life span may be connected with the short-term
517 heat-shock that was applied to both control and experimental animals in order to induce
518 forced expression of the transgene. Nevertheless, the applied heat-shock lasted only 30

519 minutes in the L1 larval stage and the life span of control animals subjected to the short-
520 term heat-shock did not differ from the normal life span of animals kept under similar
521 laboratory conditions but not subjected to the experimental heat-shock. Involvement of
522 ALKB-8 in other kinds of stress is supported by the known role of AlkB proteins in the
523 stress response. The founding member of the protein family, the bacterial AlkB is
524 involved in the DNA damage-induced stress (Fedeles et al. 2015) (Fedeles, Singh et al.
525 2015). ALKBH8 is known to regulate the rate of translation of thioredoxin reductase
526 (Endres et al. 2015) which is one of the main enzymes important for dealing with
527 oxidative stress (Li et al. 2012; Cunniff et al. 2014).

528 Our results as well as published data (Pastore et al. 2012) indicate the cytoplasm as
529 the primary place of ALKB-8 action although a low level of nuclear ALKB-8 cannot be
530 ruled out. *alkb-8* is organized in chromosome III in a hybrid operon CEOP3136. As
531 such, it is trans-spliced with both SL1 and SL2 splice leaders indicating that part of the
532 expressed forms of *alkb-8* depend on the operon promoter and the other part on the
533 internal *alkb-8* promoter. The expressional pattern of the transgene expressed under the
534 regulation of the operon promoter (used in our study) is very similar if not identical with
535 the data reported for the internal *alkb-8* promoter (Pastore et al. 2012). Our experiments
536 as well as the data reported by Wormbase (WS263) (Byrne et al. 2007) detected *alkb-8*
537 expression in intestinal cells. It is therefore likely that the effect of *alkb-8* inhibition and
538 overexpression is at least partially caused by intestinal ALKB-8.

539 ALKB-8 (from amino acid position 362 to the end) shows significant homology to a
540 yeast methyl transferase TRM9 (TRM9_YEAST) not only in the SAM binding part but
541 also at the C-terminus. Deletion of TRM9 significantly increased life span in
542 Saccharomyces cerevisiae (Fabrizio et al. 2010) suggesting that ALKB-8 may act in the

543 same pathway as the *C. elegans* orthologue of TRM9 (although in opposite ways).
544 TRM9 is predicted to be important to protect cells against protein stress (Patil et al.
545 2012). In *C. elegans* (and in most sequenced animal species), there is another gene that
546 is similar to AlkB8, that only has the methyl transferase domain, not the demethylase
547 domain C35D10.12 (NP_497751.1) but nothing is known about its function.

548 Our study shows that ALKB-8 regulates the function of the intracellular
549 compartment that can be visualized by *in vivo* Nile red staining (Ashrafi et al. 2003) that
550 forms a distinct class of lysosome related organelles (Soukas et al. 2013).

551 **Acknowledgements**

552 The wild type N2 *C. elegans* were provided by the CGC, which is funded by NIH
553 Office of Research Infrastructure Programs (P40 OD010440). Authors thank Dr.
554 Andrew Fire for vectors pPD49.78 and pPD49.83, Dr. Zdeněk Kostrouch and Dr.
555 Vladimír Saudek for advice and critical reading of manuscript. This work was supported
556 by the European Regional Development Fund "BIOCEV- Biotechnology and
557 Biomedicine Centre of the Academy of Sciences and Charles University in Vestec"
558 (CZ.1.05/ 1.1.00/02.0109) and the LQ1604 National Sustainability Program II (Project
559 BIOCEV-FAR) and the project Biocev (CZ.1.05/1.1.00/ 02.0109) from the Ministry of
560 Education, Youth and Sports of Czech Republic; PROGRES Q26/LF1 and PROGRES
561 Q28 "Oncology" from Charles University in Prague; grant SVV 260377 from Charles
562 University in Prague. The imaging was done at the Imaging Methods Core Facility at
563 Biocev, Faculty of Science, Charles University, supported by the Czech-BioImaging
564 large RI project (LM2015062 funded by MEYS CR). AB acknowledges the support by
565 the MEYS CR (CZ.02.1.01/ 0.0/0.0/16 013/0001775 Czech-Bioimaging).

References

Aravind L, and Koonin EV. 2001. The DNA-repair protein AlkB, EGL-9, and leprecan define new families of 2-oxoglutarate- and iron-dependent dioxygenases. *Genome Biol* 2:RESEARCH0007.

Ashrafi K, Chang FY, Watts JL, Fraser AG, Kamath RS, Ahringer J, and Ruvkun G. 2003. Genome-wide RNAi analysis of Caenorhabditis elegans fat regulatory genes. *Nature* 421:268-272. 10.1038/nature01279

Brenner S. 1974. The genetics of Caenorhabditis elegans. *Genetics* 77:71-94.

Buettner C, Harney JW, and Berry MJ. 1999. The Caenorhabditis elegans homologue of thioredoxin reductase contains a selenocysteine insertion sequence (SECIS) element that differs from mammalian SECIS elements but directs selenocysteine incorporation. *J Biol Chem* 274:21598-21602.

Byrne AB, Weirauch MT, Wong V, Koeva M, Dixon SJ, Stuart JM, and Roy PJ. 2007. A global analysis of genetic interactions in Caenorhabditis elegans. *J Biol* 6:8. 10.1186/jbiol58

Chan CT, Dyavaiah M, DeMott MS, Taghizadeh K, Dedon PC, and Begley TJ. 2010. A quantitative systems approach reveals dynamic control of tRNA modifications during cellular stress. *PLoS Genet* 6:e1001247. 10.1371/journal.pgen.1001247

Chan CT, Pang YL, Deng W, Babu IR, Dyavaiah M, Begley TJ, and Dedon PC. 2012. Reprogramming of tRNA modifications controls the oxidative stress response by codon-biased translation of proteins. *Nat Commun* 3:937. 10.1038/ncomms1938

Church C, Moir L, McMurray F, Girard C, Banks GT, Teboul L, Wells S, Bruning JC, Nolan PM, Ashcroft FM, and Cox RD. 2010. Overexpression of Fto leads to increased food intake and results in obesity. *Nat Genet* 42:1086-1092. 10.1038/ng.713

Cunniff B, Snider GW, Fredette N, Stumpff J, Hondal RJ, and Heintz NH. 2014. Resolution of oxidative stress by thioredoxin reductase: Cysteine versus selenocysteine. *Redox Biol* 2:475-484. 10.1016/j.redox.2014.01.021

Deng W, Babu IR, Su D, Yin S, Begley TJ, and Dedon PC. 2015. Trm9-Catalyzed tRNA Modifications Regulate Global Protein Expression by Codon-Biased Translation. *PLoS Genet* 11:e1005706. 10.1371/journal.pgen.1005706

Endres L, Begley U, Clark R, Gu C, Dziergowska A, Malkiewicz A, Melendez JA, Dedon PC, and Begley TJ. 2015. Alkbh8 Regulates Selenocysteine-Protein Expression to Protect against Reactive Oxygen Species Damage. *PLoS One* 10:e0131335. 10.1371/journal.pone.0131335

Fabrizio P, Hoon S, Shamalnasab M, Galbani A, Wei M, Giaever G, Nislow C, and Longo VD. 2010. Genome-wide screen in Saccharomyces cerevisiae identifies vacuolar protein sorting, autophagy, biosynthetic, and tRNA methylation genes involved in life span regulation. *PLoS Genet* 6:e1001024. 10.1371/journal.pgen.1001024

Fedeles BI, Singh V, Delaney JC, Li D, and Essigmann JM. 2015. The AlkB Family of Fe(II)/alpha-Ketoglutarate-dependent Dioxygenases: Repairing Nucleic Acid Alkylation Damage and Beyond. *J Biol Chem* 290:20734-20742. 10.1074/jbc.R115.656462

Fire A, Xu S, Montgomery MK, Kostas SA, Driver SE, and Mello CC. 1998. Potent and specific genetic interference by double-stranded RNA in Caenorhabditis elegans. *Nature* 391:806-811. 10.1038/35888

612 Frayling TM, Timpson NJ, Weedon MN, Zeggini E, Freathy RM, Lindgren CM, Perry JR, Elliott KS,
613 Lango H, Rayner NW, Shields B, Harries LW, Barrett JC, Ellard S, Groves CJ, Knight B,
614 Patch AM, Ness AR, Ebrahim S, Lawlor DA, Ring SM, Ben-Shlomo Y, Jarvelin MR, Sovio
615 U, Bennett AJ, Melzer D, Ferrucci L, Loos RJ, Barroso I, Wareham NJ, Karpe F, Owen KR,
616 Cardon LR, Walker M, Hitman GA, Palmer CN, Doney AS, Morris AD, Smith GD,
617 Hattersley AT, and McCarthy MI. 2007. A common variant in the FTO gene is associated
618 with body mass index and predisposes to childhood and adult obesity. *Science*
619 316:889-894.
620 Fu D, Brophy JA, Chan CT, Atmore KA, Begley U, Paules RS, Dedon PC, Begley TJ, and Samson LD.
621 2010a. Human AlkB homolog ABH8 Is a tRNA methyltransferase required for wobble
622 uridine modification and DNA damage survival. *Mol Cell Biol* 30:2449-2459.
623 10.1128/MCB.01604-09
624 Fu Y, Dai Q, Zhang W, Ren J, Pan T, and He C. 2010b. The AlkB domain of mammalian ABH8
625 catalyzes hydroxylation of 5-methoxycarbonylmethyluridine at the wobble position of
626 tRNA. *Angew Chem Int Ed Engl* 49:8885-8888.
627 Gerken T, Girard CA, Tung YC, Webby CJ, Saudek V, Hewitson KS, Yeo GS, McDonough MA,
628 Cunliffe S, McNeill LA, Galvanovskis J, Rorsman P, Robins P, Prieur X, Coll AP, Ma M,
629 Jovanovic Z, Farooqi IS, Sedgwick B, Barroso I, Lindahl T, Ponting CP, Ashcroft FM,
630 O'Rahilly S, and Schofield CJ. 2007. The obesity-associated FTO gene encodes a 2-
631 oxoglutarate-dependent nucleic acid demethylase. *Science* 318:1469-1472.
632 Gu C, Begley TJ, and Dedon PC. 2014. tRNA modifications regulate translation during cellular
633 stress. *FEBS Lett* 588:4287-4296. 10.1016/j.febslet.2014.09.038
634 Jee C, Vanoaica L, Lee J, Park BJ, and Ahnn J. 2005. Thioredoxin is related to life span regulation
635 and oxidative stress response in Caenorhabditis elegans. *Genes Cells* 10:1203-1210.
636 10.1111/j.1365-2443.2005.00913.x
637 Kalhor HR, and Clarke S. 2003. Novel methyltransferase for modified uridine residues at the
638 wobble position of tRNA. *Mol Cell Biol* 23:9283-9292.
639 Leihne V, Kirpekar F, Vagbo CB, van den Born E, Krokan HE, Grini PE, Meza TJ, and Falnes PO.
640 2011. Roles of Trm9- and ALKBH8-like proteins in the formation of modified wobble
641 uridines in Arabidopsis tRNA. *Nucleic Acids Res* 39:7688-7701. 10.1093/nar/gkr406
642 Li W, Bandyopadhyay J, Hwaang HS, Park BJ, Cho JH, Lee JI, Ahnn J, and Lee SK. 2012. Two
643 thioredoxin reductases, trxr-1 and trxr-2, have differential physiological roles in
644 Caenorhabditis elegans. *Mol Cells* 34:209-218. 10.1007/s10059-012-0155-6
645 Miranda-Vizuete A, Fierro Gonzalez JC, Gahmon G, Burghoorn J, Navas P, and Swoboda P. 2006.
646 Lifespan decrease in a Caenorhabditis elegans mutant lacking TRX-1, a thioredoxin
647 expressed in ASJ sensory neurons. *FEBS Lett* 580:484-490.
648 10.1016/j.febslet.2005.12.046
649 Pastore C, Topalidou I, Forouhar F, Yan AC, Levy M, and Hunt JF. 2012. Crystal structure and RNA
650 binding properties of the RNA recognition motif (RRM) and AlkB domains in human
651 AlkB homolog 8 (ABH8), an enzyme catalyzing tRNA hypermodification. *J Biol Chem*
652 287:2130-2143. 10.1074/jbc.M111.286187
653 Patil A, Chan CT, Dyavaiah M, Rooney JP, Dedon PC, and Begley TJ. 2012. Translational infidelity-
654 induced protein stress results from a deficiency in Trm9-catalyzed tRNA modifications.
655 *RNA Biol* 9:990-1001. 10.4161/rna.20531
656 Peters T, Ausmeier K, and Ruther U. 1999. Cloning of Fatso (Fto), a novel gene deleted by the
657 Fused toes (Ft) mouse mutation. *Mamm Genome* 10:983-986.
658 Porta-de-la-Riva M, Fontrodona L, Villanueva A, and Ceron J. 2012. Basic Caenorhabditis
659 elegans methods: synchronization and observation. *J Vis Exp*:e4019. 10.3791/4019
660 Shimada K, Nakamura M, Anai S, De Velasco M, Tanaka M, Tsujikawa K, Ouji Y, and Konishi N.
661 2009. A novel human AlkB homologue, ALKBH8, contributes to human bladder cancer
662 progression. *Cancer Res* 69:3157-3164.

Simmer F, Tijsterman M, Parrish S, Koushika SP, Nonet ML, Fire A, Ahringer J, and Plasterk RH. 2002. Loss of the putative RNA-directed RNA polymerase RRF-3 makes C. elegans hypersensitive to RNAi. *Curr Biol* 12:1317-1319.

Smemo S, Tena JJ, Kim KH, Gamazon ER, Sakabe NJ, Gomez-Marin C, Aneas I, Credidio FL, Sobreira DR, Wasserman NF, Lee JH, Puviindran V, Tam D, Shen M, Son JE, Vakili NA, Sung HK, Naranjo S, Acemel RD, Manzanares M, Nagy A, Cox NJ, Hui CC, Gomez-Skarmeta JL, and Nobrega MA. 2014. Obesity-associated variants within FTO form long-range functional connections with IRX3. *Nature* 507:371-375. 10.1038/nature13138

Songe-Moller L, van den Born E, Leihne V, Vagbo CB, Kristoffersen T, Krokan HE, Kirpekar F, Falnes PO, and Klungland A. 2010. Mammalian ALKBH8 possesses tRNA methyltransferase activity required for the biogenesis of multiple wobble uridine modifications implicated in translational decoding. *Mol Cell Biol* 30:1814-1827.

Soukas AA, Carr CE, and Ruvkun G. 2013. Genetic regulation of Caenorhabditis elegans lysosome related organelle function. *PLoS Genet* 9:e1003908. 10.1371/journal.pgen.1003908

Tabara H, Sarkissian M, Kelly WG, Fleenor J, Grishok A, Timmons L, Fire A, and Mello CC. 1999. The rde-1 gene, RNA interference, and transposon silencing in C. elegans. *Cell* 99:123-132.

Timmons L, Court DL, and Fire A. 2001. Ingestion of bacterially expressed dsRNAs can produce specific and potent genetic interference in Caenorhabditis elegans. *Gene* 263:103-112.

van den Born E, Vagbo CB, Songe-Moller L, Leihne V, Lien GF, Leszczynska G, Malkiewicz A, Krokan HE, Kirpekar F, Klungland A, and Falnes PO. 2011. ALKBH8-mediated formation of a novel diastereomeric pair of wobble nucleosides in mammalian tRNA. *Nat Commun* 2:172. 10.1038/ncomms1173

Van Gilst MR, Hadjivassiliou H, and Yamamoto KR. 2005. A Caenorhabditis elegans nutrient response system partially dependent on nuclear receptor NHR-49. *Proc Natl Acad Sci U S A* 102:13496-13501. 10.1073/pnas.0506234102

Vohanka J, Simeckova K, Machalova E, Behensky F, Krause MW, Kostrouch Z, and Kostrouchova M. 2010. Diversification of fasting regulated transcription in a cluster of duplicated nuclear hormone receptors in C. elegans. *Gene Expr Patterns* 10:227-236. 10.1016/j.gep.2010.05.001

Wilhelm T, Byrne J, Medina R, Kolundzic E, Geisinger J, Hajduskova M, Tursun B, and Richly H. 2017. Neuronal inhibition of the autophagy nucleation complex extends life span in post-reproductive C. elegans. *Genes Dev* 31:1561-1572. 10.1101/gad.301648.117

Yajnik CS, Janipalli CS, Bhaskar S, Kulkarni SR, Freathy RM, Prakash S, Mani KR, Weedon MN, Kale SD, Deshpande J, Krishnaveni GV, Veena SR, Fall CH, McCarthy MI, Frayling TM, Hattersley AT, and Chandak GR. 2009. FTO gene variants are strongly associated with type 2 diabetes in South Asian Indians. *Diabetologia* 52:247-252. 10.1007/s00125-008-1186-6

Zdzalik D, Vagbo CB, Kirpekar F, Davydova E, Puscian A, Maciejewska AM, Krokan HE, Klungland A, Tudek B, van den Born E, and Falnes PO. 2014. Protozoan ALKBH8 oxygenases display both DNA repair and tRNA modification activities. *PLoS One* 9:e98729. 10.1371/journal.pone.0098729

OPEN ACCESS Freely available online

PLOS ONE

GEI-8, a Homologue of Vertebrate Nuclear Receptor Corepressor NCoR/SMRT, Regulates Gonad Development and Neuronal Functions in *Caenorhabditis elegans*

Pavol Mikoláš[1], Johana Kollárová[2], Kateřina Šebková[1], Vladimír Saudek[2], Petr Yilma[2], Markéta Kostrouchová[2], Michael W. Krause[3], Zdenek Kostrouch[2], Marta Kostrouchová[1]*

1 Laboratory of Molecular Biology and Genetics, Institute of Cellular Biology and Pathology, First Faculty of Medicine, Charles University in Prague, Prague, Czech Republic, **2** Laboratory of Molecular Pathology, Institute of Cellular Biology and Pathology, First Faculty of Medicine, Charles University in Prague, Prague, Czech Republic, **3** Laboratory of Molecular Biology, National Institute of Diabetes and Digestive and Kidney Diseases, National Institutes of Health, Bethesda, Maryland, United States of America

Abstract

NCoR and SMRT are two paralogous vertebrate proteins that function as corepressors with unliganded nuclear receptors. Although *C. elegans* has a large number of nuclear receptors, orthologues of the corepressors NCoR and SMRT have not unambiguously been identified in *Drosophila* or *C. elegans*. Here, we identify GEI-8 as the closest homologue of NCoR and SMRT in *C. elegans* and demonstrate that GEI-8 is expressed as at least two isoforms throughout development in multiple tissues, including neurons, muscle and intestinal cells. We demonstrate that a homozygous deletion within the *gei-8* coding region, which is predicted to encode a truncated protein lacking the predicted NR domain, results in severe mutant phenotypes with developmental defects, slow movement and growth, arrested gonadogenesis and defects in cholinergic neurotransmission. Whole genome expression analysis by microarrays identified sets of de-regulated genes consistent with both the observed mutant phenotypes and a role of GEI-8 in regulating transcription. Interestingly, the upregulated transcripts included a predicted mitochondrial sulfide:quinine reductase encoded by Y9C9A.16. This locus also contains non-coding, 21-U RNAs of the piRNA class. Inhibition of the expression of the region coding for 21-U RNAs leads to irregular gonadogenesis in the homozygous *gei-8* mutants, but not in an otherwise wild-type background, suggesting that GEI-8 may function in concert with the 21-U RNAs to regulate gonadogenesis. Our results confirm that GEI-8 is the orthologue of the vertebrate NCoR/SMRT corepressors and demonstrate important roles for this putative transcriptional corepressor in development and neuronal function.

Citation: Mikoláš P, Kollárová J, Šebková K, Saudek V, Yilma P, et al. (2013) GEI-8, a Homologue of Vertebrate Nuclear Receptor Corepressor NCoR/SMRT, Regulates Gonad Development and Neuronal Functions in *Caenorhabditis elegans*. PLoS ONE 8(3): e58462. doi:10.1371/journal.pone.0058462

Editor: Vincent Laudet, Ecole Normale Supérieure de Lyon, France

Received August 17, 2012; **Accepted** February 5, 2013; **Published** March 6, 2013

Funding: The work was supported by the following grants: grant 304/08/0970 from the Czech Science Foundation (http://www.gacr.cz/international.htm), grant 0021620806 from the Ministry of Education, Youth and Sports of the Czech Republic (http://www.msmt.cz), Prvouk/1LF/1 and UNCE 204022 from the Charles University in Prague (http://www.cuni.cz). PM, JK and KS were partially supported by the grant SVV 2012 264514 from the Charles University in Prague (http://www.cuni.cz). KS was partially supported by the Grant 579612 from the Charles University in Prague. MWK is supported by the Intramural Research Program of the National Institute of Diabetes and Digestive and Kidney Diseases (NIDDK) of the National Institutes of Health, USA (http://www2.niddk.nih.gov). The funders had no role in study design, data collection and analysis, decision to publish, or preparation of the manuscript. No additional external funding received for this study.

Competing Interests: The authors have declared that no competing interests exist.

* E-mail: marta.kostrouchova@lf1.cuni.cz

Introduction

NCoR and SMRT are paralogous vertebrate proteins that were first identified as transcriptional corepressors interacting with unliganded thyroid and retinoid receptors [1,2]. Both NCoR (a.k.a. NCoR1, NCOR1) and SMRT (a.k.a. NCoR2, NCOR2) knockouts in mice are embryonic lethal suggesting that their regulatory roles are indispensable for normal development [3]. NCoR/SMRT function occurs through the assembly of a repressor complex composed of nuclear hormone receptors (NHRs), histone deactylases (HDACs), and other components [4]. Chromatin remodeling depends on the formation of a stoichiometric complex between SMRT/NCoR and HDAC3 that is mediated by two SANT (a.k.a. MYB) domains located at the N-terminus of NCoR/SMRT. Such domains are present in many nuclear receptor corepressors and related proteins and consist of three alpha-helices folded around a core of three hydrophobic amino acids, which determines its characteristic spatial structure [5–7]. The N-terminus proximal SANT1 domain activates the HDAC3 deacetylase [8,9] and is referred to as the deacetylase activation domain (DAD). A prominent feature of all DAD domains is the absolutely conserved lysine residue (K449 in human SMRT) that promotes HDAC3 activation but not its binding to the complex. The second SANT domain, SANT2, binds unacetylated histone H4 and increases affinity of NCoR/SMRT to HDAC3, suggesting a role for this motif in stabilizing the deacetylated histone tail and blocking its subsequent acetylation [7,8]. While the SANT2 domain in NCoR/SMRT possesses all of the typical features of a general SANT domain, the presence and structure of the SANT1 domain is unique to NCoR/SMRT and its orthologues [10]. The SANT1 domain contains a characteristic irregular N-

terminal helix that is important for forming an additional surface hydrophobic groove that contributes to the interaction with HDAC3. Thus, there are multiple diagnostic domains and amino acid residues that can distinguish NCoR/SMRT orthologues from more general SANT domain-containing proteins.

Although homologues of NCoR/SMRT can be easily identified across vertebrate species, obvious homologues of these corepressors were difficult to identify by sequence homology in either *Drosophila* or *C. elegans*. This is surprising in light of the identification of clear sequence homologues for other NCoR/SMRT corepressor complex components in flies and worms such as the histone deacetylase complex associated factors NuRD and SIN3 [11,12]. We have taken a bioinformatics approach focusing on the unique features of NCoR/SMRT to identify GEI-8 as a possible NCoR/SMRT homologue in *C. elegans*; Yamamato and colleagues came to the same conclusion while this work was in progress [13]. GEI-8 was originally identified as a GEX-3 binding protein based on yeast-two-hybrid assays [14]; no RNAi phenotypes or functions for GEI-8 have previously been described. We have analyzed the expression of *gei-8* and studied its function using a putative null allele with a large deletion in the *gei-8* coding sequence resulting in a truncated protein product due to a novel stop codon; this truncated product lacks the domain involved in binding of nuclear receptors (NR domain, a.k.a CoRNR box [15]). Our mutant studies demonstrate a role for GEI-8 in development and suggest it is specifically required for germline development and proper cholinergic regulation. Our whole genome expression analysis demonstrates that GEI-8 is required for transcriptional regulation, consistent with its function and orthology to mammalian NCoR/SMRT corepressors.

Results

Sequence Analysis

In an effort to identify homologues of NCoR/SMRT in the *C. elegans* proteome, we performed BLAST and PSI-BLAST searches in multiple protein databases [16,17]. Searches with human NCoR and SMRT sequences returned the sequence annotated as GEI-8 (UniProt GEI8_CAEEL, E value 2e-10), as the best hit. In the reciprocal BLAST, NCoR and SMRT appeared likewise as the best hits for GEI-8 within the human proteome. Although only a small fraction of the entire protein sequence (~7%) was retrieved by Blast searches, nearly complete protein sequences were recovered in PSI-BLAST after the third iteration. Six GEI-8-related proteins from other Nematoda species (*C. elegans, C. brenneri, C. briggsae, C. remanei, C. japonica, Loa loa* and *Brugia malayi*) were aligned and submitted as a query in PSI-BLAST (**Figure 1**). Sequences were extracted from databases UniProt, Wormbase and Ensembl. Entries for *C. japonica* and *X. tropicalis* were corrected according to NCBI nucleotide sequences using the GeneWise program [18]. An alignment of these nematode GEI-8-related proteins with human NCoR was obtained in the second iteration.

Multiple sequence alignments resulting from PSI-BLAST were further improved using the profile-to-profile alignment method (PSI-Coffee) [19], however, its quality remained ambiguous in several regions across the protein. All NCoR homologues contain long stretches of low complexity (e.g. 23% of amino acids in GEI-8 or 13% in human NCoR1) that are variable in length. The well conserved N-terminal region from representative *Metazoa/Fungi* NCoR/SMRT is shown in **Figure 1**. The sequence conservation in the C-terminal domains is much lower; all sequences contain many insertions, deletions, prolines, serines and oligoGlu residues that vary between species. This C-terminal variability is evident even within the alignment of the GEI-8-related proteins from the phylogenetically related *Caenorhabditis* species. We also used ClustalW2.0 for identification of putative interaction motifs near the C-terminus. NCoR and SMRT bind nuclear hormone receptors by NR-binding domains consisting of three and two CoRNR-box sequences respectively. The CoRNR-box sequence was previously defined as L.x.x.x.I.x.x.x.I/L [20]; I/L.x.x.I/V.I [21]; L/V.x.x.I/V.I [22]. We identified two putative CoRNR-box like sequences in GEI-8 (**Figure 2A**). The predicted GEI-8 sequence also contains two glutamine rich regions [23] that also might serve as interaction domains.

The most conserved N-terminal regions of the GEI-8 related sequences contain both the DAD and SANT domains with their location and the positions of the conserved helices shown in **Figure 1**. We noted that GEI-8 and related sequences preserve all features known to be essential for correct functioning of NCoR/SMRT as an HDAC-dependent transcriptional corepressor [10] (highlighted in **Figure 1**). These include the number of helices, their topology, the conserved amino acids needed for the integrity of the structure and for the interaction with HDAC and, most importantly, the K159 residue in the loop between helices H1 and H2 that is indispensable for the activation of HDAC3. The helix H0, known to be very irregular in human SMRT, is probably also present although it contains a two amino acid insertion between the second and third helical turn. Based on the sequence analysis, we concluded that GEI-8 bears all major features identified in other NCoR/SMRT orthologues in annotated genomes from other species and is the NR corepressor and NCoR/SMRT orthologue in *C. elegans*.

The C-terminal Region of GEI-8 is Capable of Binding GST-NHR-60

In order to confirm functional relatedness of GEI-8 with NCoR/SMRT, we performed a binding assay of the GEI-8 C-terminal domains to GST-NHR-60. NHR-60 is a member of a diversified subfamily of nematode receptors related to HNF-4 alpha and is important for embryonic and early larval development [24]. Mammalian HNF-4 alpha interacts both physically and functionally with SMRT [25] raising the possibility that NHR-60 may similarly interact with GEI-8. We divided the C-terminal region of *gei-8* into three domains: I. containing the NR1 binding site (position 2480–3485 in *gei-8a* isoform), II. containing the sequence between NR bindings sites (position 3413–4389) and III. containing the NR2 binding site (position 4274–5513). As expected from our sequence homology analysis of GEI-8 as it relates to NCoR/SMRT, the C-terminal region I of GEI-8 that includes the predicted NR1 binding site showed affinity to GST-NHR-60 but not to the control protein expressing the GST anchor used for pull-down experiments (**Figure S1**).

gei-8 Expression

The *C. elegans gei-8* gene is located on chromosome III and gives rise to three predicted isoforms with mRNAs ranging from 5.3 to 5.6 kb (WormBase WS195). All predicted isoforms contain two SANT domains that could provide DNA and HDAC interaction functions (**Figure 2A and B).** Using primers based on predicted cDNA sequences of *gei-8* isoforms, we cloned three overlapping regions corresponding to *gei-8* cDNAs and confirmed the expression of predicted isoform *gei-8a* containing both SANT domains and two putative CoRNR-box like motifs (**Figure 2A).** The *gei-8a* cDNA clones also revealed that exon 12 can be removed and exon 16 is modified by alternative splicing (**Figure 2A**); a spliced region of the same location and size as our cDNA clone was also detected by polyA mRNA expression profiling [26]. Depending on the presence or absence of exon 12,

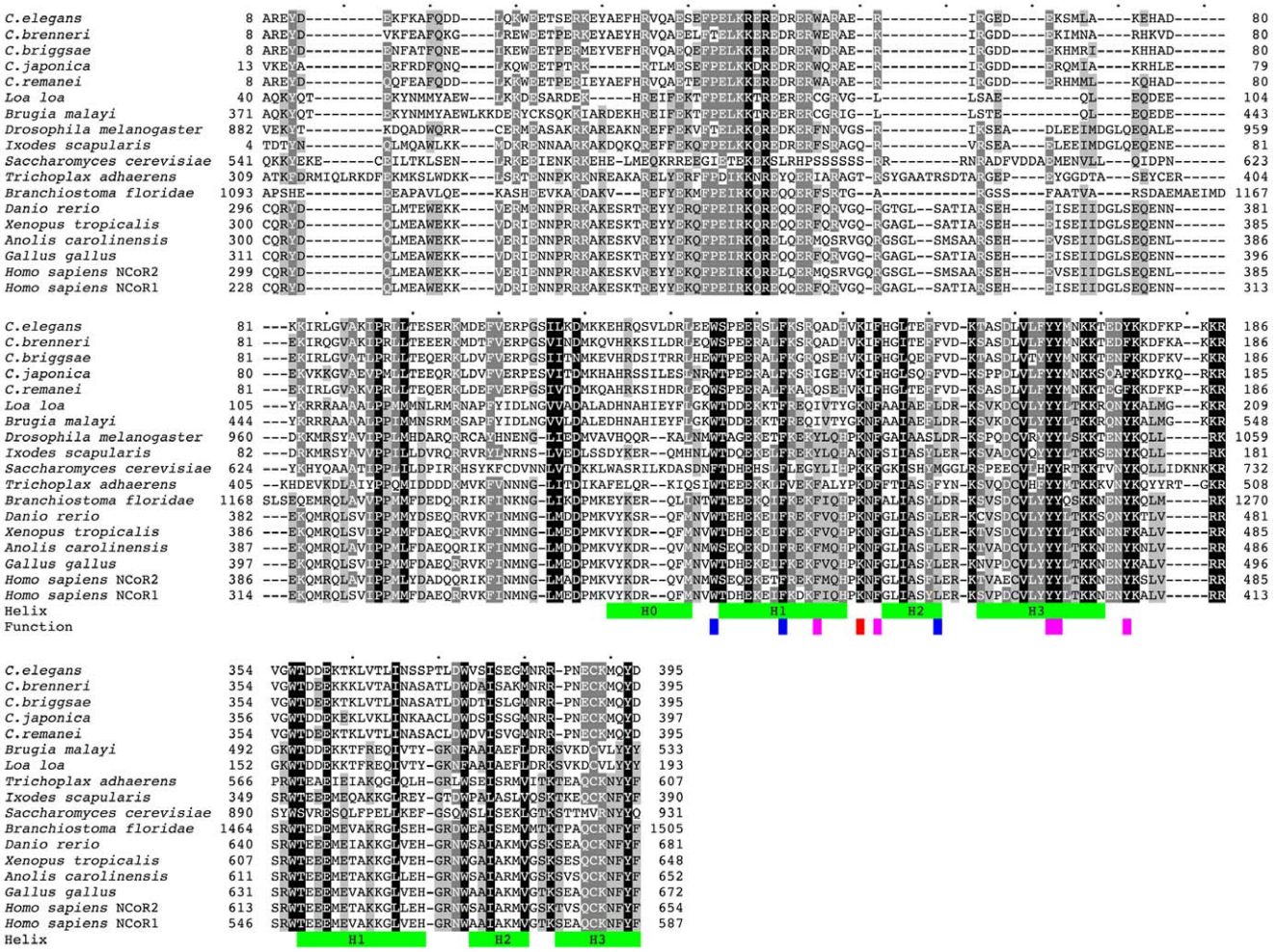

Figure 1. Comparison of N-terminal regions of GEI-8-related proteins to NCoR/SMRT. Sequence alignment of GEI-8 nematode orthologues with their nearest Metazoa/Fungi homologues, both human orthologues NCoR1 and SMRT (NCoR2) are shown. Green bars indicate the position of the alpha-helices in the structure of the upstream DAD domain of human SMRT and homology predicted positions in the second SANT domain. Residues indispensable for regulating HDAC interactions and function are highlighted in blue (needed for the structural integrity), magenta (interaction with HDAC) and red (activation of HDAC). Only the N-terminal part of the sequences is shown. The identical and similar residues are highlighted by different intensity of shading. Sequence identifiers: *C. elegans*: GEI8_CAEEL, *C. brenneri*: CN15693, *C. briggsae*: A8X8F0_CAEBR, *C. remanei*: RP40355, *C. japonica*: JA23925 ABLE03010463.1 ABLE03032768.1 ABLE03032771.1 ABLE03032769.1 ABLE03032772.1, *Loa loa*: E1FVE0_LOALO, *Brugia malayi*: A8NSC3_BRUMA, *Ixodes scapularis*: B7PZ26_IXOSC, *Saccharomyces cerevisiae*: SNT1_YEAST, *Drosophila melanogaster*: Q9VYK0_DROME, *Trichoplax adhaerens*: B3SAN1_TRIAD, *Branchiostoma floridae*: C3XV35_BRAFL, *Danio rerio*: A8B6H7_DANRE, *Xenopus tropicalis*: NCOR1_XENTR AAMC01044136.1, *Anolis carolinensis*: ANOCA15679 2 ENSACAP00000014806; ENSACAT00000015107, *Gallus gallus*: UPI0000E813A6, *Homo sapiens*: NCOR2_HUMAN (NCoR2), *Homo sapiens*: NCOR1_HUMAN (NCoR1). PDB structure 1XC5 was used to determine the position of the helices.

doi:10.1371/journal.pone.0058462.g001

the size of *gei-8* cDNA is 5043 bp (*gei-8d*) and 5292 bp (*gei-8e*), giving rise to either a 1680 or 1763 amino acid long GEI-8 isoforms. We have not cloned the region containing the complete predicted protein encoded by inclusion of exon 16, however, polyA mRNA expression profiling data suggest that this variant is expressed. We confirmed the transcription of the *gei-8a* 5′ untranslated region (5′ UTR) and its trans-splicing to SL1 by PCR assays [27]. Expression of *gei-8b* and *gei-8c* was not detected using primers directed at predicted exons 1 to 3; our results are consistent with polyA mRNA expression profiling data generated by modENCODE (**Figure 2B**) [**26**].

We quantified *gei-8* expression in individual embryonic and larval stages by real-time qPCR using cDNA prepared from synchronized populations of wild-type animals. We separately analyzed a region common for all predicted isoforms (*gei-8a, b, c*) as well as a *gei-8a*-specific region. We detected expression after probing both regions in all developmental stages at constant relative levels with the exception of the fourth larval (L4) stage where we observed a 2-fold increase for both (**Figure 3**). We concluded that *gei-8a* was expressed throughout development, with its late larval increase possibly reflecting expression in the maturing germline.

The spatial expression pattern of *gei-8* was studied using three different *gei-8::gfp* constructs based on the predicted start of transcription for *gei-8b* (promoter 1), the detected start of transcription for *gei-8a* (promoter 2), and an overlapping region covering both promoters (promoter 3) (**Figure 2C**). pPD95.69 and pPD95.67 promoterless, nuclear localization signal-containing vectors were used for the promoter 1 and promoter 2 constructs,

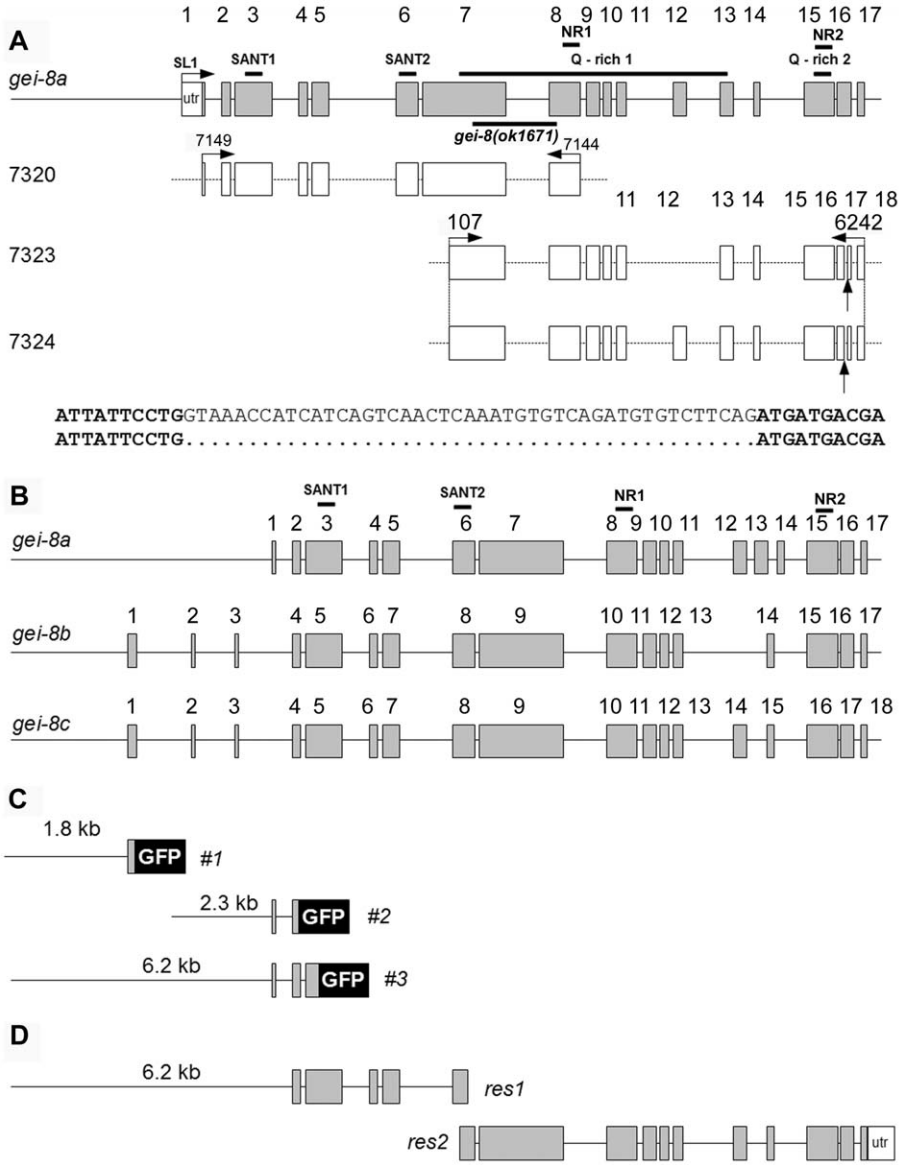

Figure 2. Expression analysis of *gei-8*. (**A**) Schematic representation of the predicted *gei-8a* isoform consisting of 17 exons compared with detected expression. cDNA clones 7320, 7323 and 7324 are indicated with their exons (open rectangles). Expression of exon 12 and 16 is not constant. Exon 12 in cDNA clone 7323 and 45 bp from exon 16 in cDNAs 7323 and 7324 were removed by alternative splicing (bottom two lines). The location of predicted SANT and glutamine-rich interaction domains is marked by lines above the *gei-8a* diagram. Location of *gei-8(ok1671)* mutation used in expression analysis is marked by a line below the *gei-8a* diagram. Two regions identified as putative CoRNR nuclear receptor binding motifs are indicated in the exon 8 and 15 (NR). (**B**) Schematic representation of predicted *gei-8* isoforms *a, b* and *c*. (**C**) GFP reporter gene constructs #1, #2 and #3 used for expression analysis. (**D**) Overlapping regions of *gei-8* gDNA used for rescue. The size of the overlapping region is 191 bp.
doi:10.1371/journal.pone.0058462.g002

respectively. Expression from promoter 3 was studied by the PCR fusion-based SOEing approach [28].

The promoter 1 reporter gene consisted of 1.8 kb upstream of the predicted *gei-8b* start codon and 222 bps of predicted exon 1. Its expression started in embryos at the comma stage in a ubiquitous pattern and was present in all larval stages. In larvae, the expression was detected in pharyngeal and tail neurons, intestinal cells, egg-laying muscles and the anal depressor (**Figure 4**). The promoter 2 reporter gene construct consisted of 2.3 kb upstream of the predicted *gei-8a* start codon and included exon 1 and 64 bp of exon 2. The expression of this reporter gene was observed in all larval stages starting at the L1 stage and continuing through adulthood where expression was primarily observed in neurons of the pharyngeal nerve ring, head neurons, tail neurons and the egg-laying muscles**.** The promoter 3 reporter gene construct contained 6.2 kb upstream of the predicted *gei-8a* start codon, covering both promoter regions 1, 2 and exons 1, 2 and a part of exon 3; GFP sequences were derived from pPD95.75 by SOEing [28] and did not contain a nuclear localization signal. Expression of this reporter gene started at the embryonic comma stage. Larval expression was detected in pharyngeal neurons, ventral and dorsal nerve cords, tail neurons, egg-laying neurons, and egg-laying muscles. In males, GFP was observed in male-specific tail ganglia and rays. Typical examples of GEI-8::GFP cell- and tissue-specific expression are shown in **Figure 4.** Taken altogether, our reporter gene expression results defined multiple

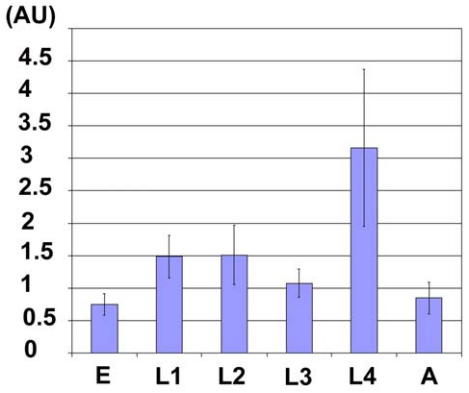

Figure 3. Normalized expression of *gei-8a*. The expression of *gei-8a* was measured for two regions (with primers 6168 and 01/042 and 6200 and 01/153) and quantitated relative to the constitutive gene *ama-1*. The expression of *gei-8a* peaks in the L4 stage. Relative expression was determined as proportion of lowest expression found in the embryonic stage and indicated as arbitrary units.
doi:10.1371/journal.pone.0058462.g003

and distinct cis-acting regulatory regions of *gei-8* that drive similar expression patterns that are present throughout development and predominantly in neurons. Expression in the germline would not be revealed by this strategy because transgenes are usually silenced in the germline [29]. However, we noted that *gei-8* expression in the germline has been detected by Y. Kohara's in situ hybridization results accessible in the Kohara in situ database NEXTDB (http://nematode.lab.nig.ac.jp).

Loss of *gei-8* Results in Mutant Phenotypes

We obtained the VC1213 strain harboring a *gei-8(ok1671)* deletion allele generated by the *C. elegans* Knockout Consortium. The mutation was initially characterized as a 1095 bp deletion/45 bp insertion affecting exons 7 and 8 of *gei-8a*, removing the intron between them. We verified the size and location of the deletion by PCR genomic amplification from mutant animals and showed that the inserted sequences are identical to a 45 bp region from exon 7 starting at position 1550 of the predicted *gei-8a* isoform cDNA sequence. Sequencing the *gei-8(ok1671)* cDNA revealed a stop codon present in the *gei-8(ok1671)* transcript at position 663, giving rise to a predicted protein containing SANT1 and SANT2 domains, but missing the majority of the putative NR interaction sites at the C-terminus of the protein. The mutant mRNA was detected in homozygous *gei-8(ok1671)* animals using RT-PCR at levels similar to wild-type animals, suggesting the premature stop codon may be bypassed in some transcripts by alternative splicing or that the premature stop codon is not efficiently recognized by nonsense mediated decay [30]. Thus, truncated GEI-8 protein may be present in homozygous mutant larvae.

The homozygous *gei-8(ok1671)* animals had obvious phenotypes, including a progressive defect in locomotion starting at the L2 stage that was marked by a delayed response to prodding and a low pharyngeal pumping rate (**Figure 5**). Compared to wild-type animals of the same age, mutants were also characterized by a shorter maximum body length (750.25 μm, n = 6, SD = 50.59 μm), a convoluted intestine, gonadogenesis defects including loss of the spermathecae, sterility, and arrest at the L4 stage of development (**Figure 6 C and D**). After outcrossing the original mutant strain to wild-type animals, the heterozygous mutant strain segregated 26.2% (SD = 2.4; n = 2656) affected progeny as described (**Table 1**). To verify that the observed phenotypes were caused by the *ok1671* deletion allele of *gei-8*, we performed rescue using intact *gei-8* genomic DNA. This method has been used previously to generate transgenic animals and to rescue mutant animals [31–34]. Overlapping PCR regions containing a 6 kb putative promoter region plus the complete coding region of *gei-8a* (**Figure 2D**) were injected into heterozygous *gei-8(ok1671)* animals along with pRF4 injection marker, rollers were selected and their progeny were screened for locomotion defects as defined as impaired responses to prodding. The wild-type *gei-8* genomic sequences were able to reduce the percentage of affected mutant progeny segregating from heterozygous hermaphrodites from 26.2% to 18.3% (SD = 3.4; n = 7883); this difference was significant using the Student's *t*-test ($p<0.001$; SD = 3.16) (**Table 1**). Importantly, all other mutant phenotypes also showed improvement in the presence of wild-type genomic sequences leading us to conclude that most, if not all, of the defects we observed in *gei-8(ok1671)* animals were due to disruption of GEI-8 activity.

We scored 20 *gei-8(ok1671)* mutant animals for germline development defects using Nomarski optics and DAPI (4',6-diamidino-2-phenylindole) staining of fixed animals. In 19/20 mutant animals examined, distal tip cell (DTC) migration stopped short, reaching only two thirds of it's normal length of migration on the dorsal side of the animal (**Figure 6C and D**). In homozygous mutant animals, both gonad arms were underdeveloped, containing fewer meiotic nuclei and germ cells compared to wild-type and heterozygous *gei-8(ok1671)* control animals. We also failed to detect spermathecae, sperm, or embryos in any mutant animals. We concluded that *gei-8(ok1671)* mutant germlines are arrested at the L4 stage, before complete gonad elongation and spermatheca development, although some somatic markers of early young adult stages were already present (adult alae, adult vulva)**.** The arrested animals also had a shorter lifespan than wild-type controls. The average lifespan of *gei-8(ok1671)* mutants at 20°C was 11 days (n = 21, SD = 3.4), which was significantly shorter than the average lifespan of wild type controls (17.4 days, n = 12, SD = 3.9).

Two muscle-related phenotypes were observed in homozygous *gei-8(ok1671)* mutants; decreased locomotion on plates and decreased pharyngeal pumping rates. The locomotion defects we observed for *gei-8(ok1671)* animals on plates prompted us to carry out a thrashing assay. When placed in liquid, wild-type animals bend back and forth moving their head and tail relative to the midbody of the animal in a thrashing motion that can be easily quantitated [35]. In the *gei-8(ok1671)* mutant strain, this natural thrashing behavior is impaired and deteriorated over the course of development. Unlike wild-type controls, homozygous *gei-8(ok1671)* mutants at the L4 stage were not able to perform smooth thrashing. Instead, their movements were spastic and irregular, averaging only 0 to 6 bends per minute at the L4 stage compared to about 250 bends per minute for wild-type animals (n = 10). Similarly, assays of pharyngeal pumping revealed irregular and reduced contraction rates in the homozygous mutants that became progressively worse with age. The average pumping rate in *gei-8(ok1671)* homozygous animals was 31.8, 17.5 and 5.3 pumps per minute at L2, L3 and L4 stages, respectively (n = 10 for each larval stage), compared to 250 pumps per minute for wild-type animals.

The movement and pharyngeal mutant phenotypes could be due to defects in the functioning of muscle, nerves, or both. To investigate muscle structure, we performed immunostaining using phalloidin and anti-MYO3 antibody directed against contractile apparatus components. Phalloidin stains actin filaments whereas the anti-MYO3 probe recognizes myosin heavy chain-3 [36,37].

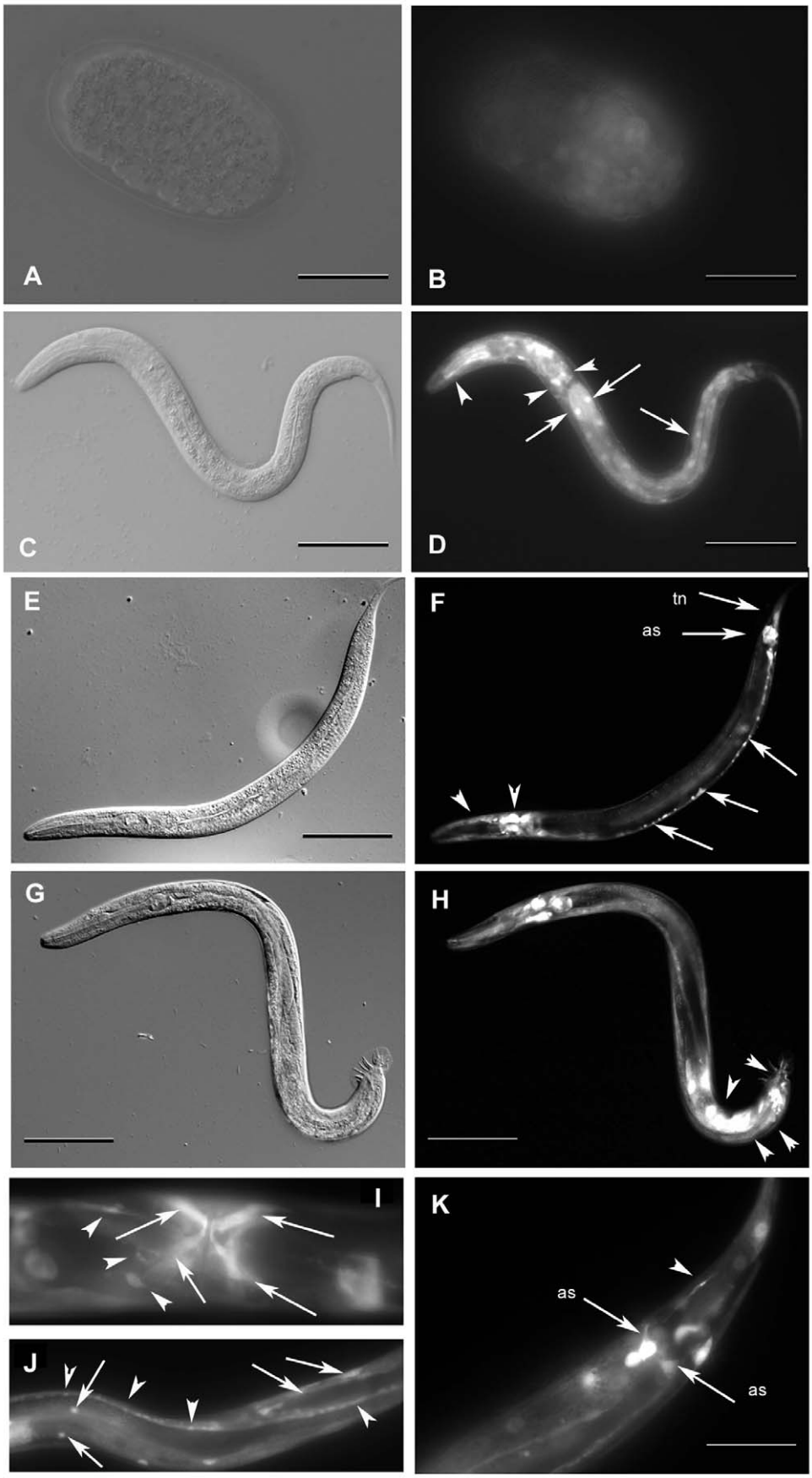
A
B
C
D
E
F
tn
as
G
H
I
J
K
as
as

Figure 4. Analysis of *gei-8* expression using transgenic lines. The expression of *gei-8* was studied using transgenic lines carrying three different predicted promoters (#1, #2 and #3) fused with gene coding for GFP (indicated in Figure 2C) *gei-8::GFP*. Panels B and D show the expression from promoter #1 and panels F, H, I, J and K show the expression from promoter #3. Expression from promoter #2 construct was identical with that from promoter #3 and is not shown. (**A** and **B**) Embryonic GFP expression is ubiquitously present since comma stage. (**C** and **D**) L2 larva expressing *gei-8::GFP* ubiquitously with the highest expression in the head neurons and in the neuronal ring (arrowheads) and intestinal cells (arrows). (**E** and **F**) Expression of GEI-8::GFP in pharyngeal neurons (arrowheads), ventral nerve cord (arrows), anal sphincter (arrow - as) and tail neurons (arrow - tn) of an L4 larva. (**G** and **H**) Expression of GEI-8::GFP in L4 male larva. Additional expression is seen in male specific neurons (arrowheads). (**I**) L4 larva expressing GEI-8::GFP in egg laying structures, vulval and uterine muscles (arrows), egg laying neurons (arrowheads). (**J**) GEI-8::GFP expression in somatic muscles (arrows) and nerve cord (arrowheads). (**K**) Detail of expression of GEI-8::GFP in hermaphrodite tail neuron (arrowhead) and anal sphincter (arrows - as). (Figs. **A**, **C**, **E**, **G** in Nomarski optics and **B**, **D**, **F**, **H**, **I**, **J**, **K** in fluorescence microscopy). Scale: **A**, **B**, **I**, **J** 20 µm; **C**, **D**, **E**, **F**, **G**, **H** 100 µm; **K** 50 µm.
doi:10.1371/journal.pone.0058462.g004

Immunostaining revealed no obvious structural differences between *gei-8(ok1671)* mutants and wild-type controls (not shown). Yamamoto et al. reported increased mitochondrial oxidative function in *C. elegans* after *gei-8* inhibition by RNAi [13]. We confirmed that finding using MitoTracker Red to visualize the mitochondrial oxidative state; homozygous *gei-8(ok1671)* mutants had an average mean density of staining that was more than 2.7 times greater ($p<0.001$) than that observed in wild-type larvae (**Figure S2**). Elevated MitoTracker staining could also be visualized in heterozygous *gei-8(ok1671)* mutants compared to wild-type N2 worms, but was not statistically significant in densitometric analysis of randomly selected progeny of heterozygous *gei-8(ok1671)* animals with a normal phenotype (which included both heterozygous mutants as well as wild-type animals (**Figure S3**).

The absence of obvious muscle defects in *gei-8* mutants suggested that the locomotion and pharyngeal pumping defects might be due to problems in neurotransmission. We investigated synaptic transmission by assaying animal sensitivity to either aldicarb or levamisole [38,39]. Aldicarb is a reversible acetylcholinesterase inhibitor that increases the accumulation of acetylcholine in the synaptic cleft causing whole body paralysis and inhibition of pharyngeal pumping. Homozygous *gei-8(ok1671)* mutants (n = 64) and wild-type animals (n = 75) at the L4 stage were incubated on NGM plates with 1 mM aldicarb and scored over time for paralysis in three separate experiments. The onset of paralysis occurred significantly earlier in *gei-8(ok1671)* mutants than in wild-type controls (**Figure 7A**). Levamisole is a cholinergic agonist that also results in animal paralysis. We performed two experiments with homozygous *gei-8(ok1671)* mutants (n = 40) and wild-type animals (n = 40) at the L4 stage on NGM plates with levamisole at a concentration of 1 mM. As in the aldicarb assay, the onset of paralysis occurred significantly earlier in *gei-8(ok1671)* mutants compared to controls (**Figure 7B**). Taken together, these results indicate that the *gei-8(ok1671)* mutation results in abnormal cholinergic signaling, however, it does not distinguish between post-synaptic versus pre-synaptic transmission defects.

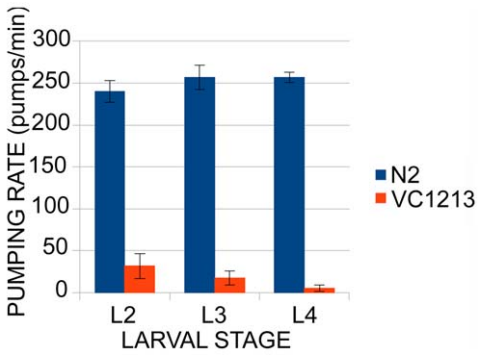

Figure 5. Analysis of the pharyngeal pumping rate of *gei-8(ok1671)* mutant animals and controls. Pharyngeal pumping rate is regulated by cholinergic transmission. In *gei-8* mutants the pumping rate is low compared to wild-type animals and decreases with age (n = 10 for each category).
doi:10.1371/journal.pone.0058462.g005

gei-8 Loss of Function Leads to Transcription Deregulation

Effects of the *gei-8(ok1671)* mutation on gene expression were studied with whole genome microarrays (Affymetrix). Changes in gene expression were defined as increased or decreased if statistically significant compared to wild-type controls in at least 2 out of 3 biological replicates. Deregulated genes were analyzed for Gene Ontology (GO) term enrichment and clustered according to functional classification using DAVID 6.7 [40] and KEGG pathway tools [41].

Expression microarray analysis revealed 756 probe sets with decreased expression, corresponding with 690 unique Wormbase IDs (**Table S1**). DAVID classification tools [40] identified 645 IDs using medium classification stringency. GO analysis resulted in 32 clusters with an enrichment score greater than 2 and $P<0.05$. The list was enriched in spliceosome (29 genes), proteasome (13 genes), cysteine and methionine metabolism (7 genes), and RNA polymerase genes (6 genes) as identified by KEGG pathway analysis. Among specific genes involved are RNA polymerase II and III (Pol II subunits B4, B7, B9 and Pol III subunits AC2 and F09F7.3), spliceosome components (U1 to U6 snRNAs, *hel-1* helicase and others), and proteasome subunits (*pas-3*, *pas-4*, *pbs-1*, *pbs-3*, *pbs-4*, *pbs-6*, *pbs-7*, *rpt-1*, *rpt-2*, *rpn-2*, *rpn-5*, *rpn-8*, *rpn-12*). The most common functional categories over represented by the changes in gene expression were growth, embryonic or larval development and development of reproductive structures. Other clusters include multiple histones and histone-like genes, mitochondrial membrane proteins, sperm structural proteins and hedgehog-like family genes. Interestingly, the set of genes down-regulated in *gei-8* mutants included several genes required for proper muscle function, including *unc-52* (myofilament assembly and/or attachment of the myofilament lattice to the cell membrane), *unc-27* (troponin I family), *unc-54* (muscle myosin class II heavy chain), *pat-10* (body wall muscle troponin C), *lev-11* (tropomyosin), *mlc-2* (myosin light-chain), and *tni-1* (troponin 1). It is unclear if such changes in muscle gene expression contribute to, or are the result of, the defective movement phenotypes we observed in *gei-8(ok1671)* mutant animals. Depletion of NCoR1 function specifically in mouse muscle resulted in increased muscle mass and mitochondrial function [13], a phenotype opposite to what we observed in worms with reduced GEI-8 activity in all tissues.

Microarray analysis revealed 296 probe sets with increased expression, corresponding to 275 unique Wormbase IDs (**Table S2**). GO analysis identified 7 clusters with an enrichment score greater than 2 and $P<0.05$. Enriched clusters included gene

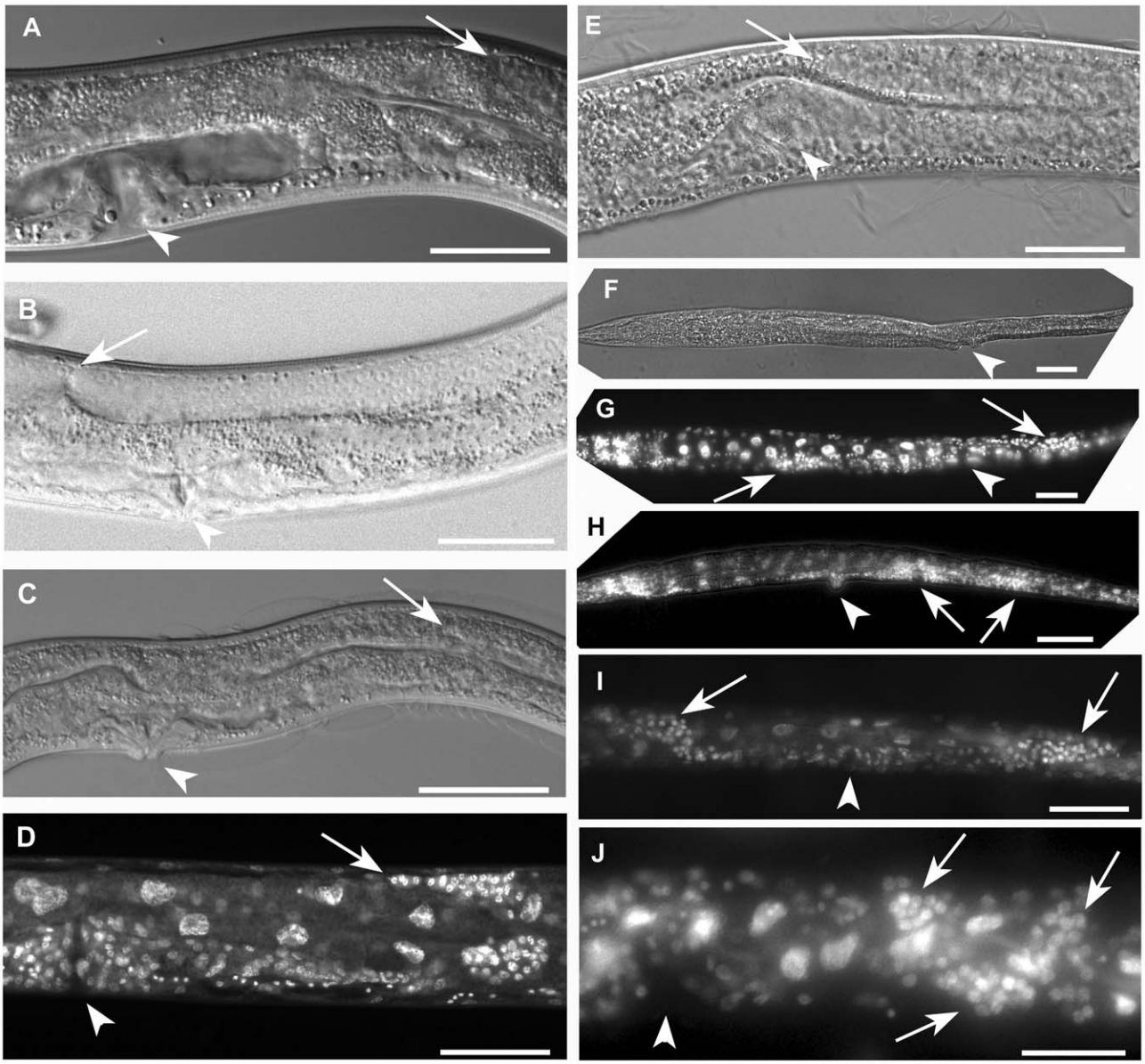

Figure 6. Development of the germline in *gei-8(ok1671)* mutants and additional phenotypic changes induced by RNAi targeted against Y9C9A.16 (*sqrd-2*) in homozygous *gei-8(ok1671)* mutants. (**A**) The reproductive structures of a wild-type larva at the L4 stage is shown. The vulva is indicated by an arrowhead and formation of the uterus is visible next to vulval structures. The position of the lead migrating cell for the gonad (distal tip cell) during the larval L4 stage is indicated by arrow. (**B**) Development of the gonad in a young adult N2 animal. The distal gonad arm continues in growth beyond the position of the vulva (marked by arrowhead) and makes contact with the proximal gonad arm (arrow). (**C**) *gei-8(ok1671)* mutant gonadogenesis by Nomarski optics. The arrested gonad arm in a position similar to wild type L4 larva is indicated by arrow. The vulva is marked by an arrowhead. (**D**) A *gei-8(ok1671)* mutant with arrested growth of the gonad as visualized by DAPI staining. The distal tip of arrested gonad is marked by an arrow and the vulva by an arrowhead. (**E**, **F**, **G**, **H**, **I** and **J**) Additional phenotypic changes induced by RNAi targeted against Y9C9A.16 (*sqrd-2*) region including three 21U-RNAs: 21ur-2020, 21ur-11733 and 21ur-9201 in *gei-8(ok1671)* homozygous mutant animals. (**E**) A *gei-8(ok1671)* mutant treated with *sqrd-2* RNAi shows growth of the gonad beyond the usual arrest point, reaching the position of the vulva (marked by arrow and arrowhead, respectively). (**F**) Additional phenotypes of *gei-8(ok1671)* animals treated with *sqrd-2* RNAi. Nomarski optics view of homozygous *gei-8(ok1671)* larva treated with *sqrd-2* RNAi revealing frequent growth defects, including irregular body shapes, (distention of proximal part of the body and thin elongation of the distal part of the body) and extended growth of the distal part of the gonad. The gonad is visualized by DAPI staining in panel **G** (distal arm of the gonad is marked by right arrow, proximal arm of the gonad is marked by left arrow). Arrowhead indicates the position of vulva in panels E, F and G. (**H**) Additional growth defects induced by *sqrd-2* RNAi in homozygous *gei-8(ok1671)* worms including a Pvul phenotype (arrowhead), accumulation of gonadal cells with a possible incomplete second vulva formation (left arrow) and a distal arm of germline that fails to turn and instead continues to grow in the direction of the thin and elongated tail (right arrow). (**I**) A mutant animal with germline growth directional changes of both gonad arms induced by *sqrd-2* RNAi: anterior gonad arm makes an incomplete turn dorsally and continues to grow in the anterior direction (left arrow) while the posterior gonad arm fails to turn and continues in additional growth towards the tail (right arrow). The position of vulva is indicated by arrowhead. (**J**) A homozygous *gei-8(ok1671)* mutant developing a convoluted irregular accumulation of cells of distal gonad arm in the position of gonad turn (marked by arrows). The position of vulva is indicated by arrowhead. Scale **A**, **B**, **D**, **E** and **J** 50 μm, **C**, **F**, **G**, **H** an **I** 100 μm.

doi:10.1371/journal.pone.0058462.g006

Table 1. Rescue experiment of *gei-8(ok1671)* with overlapping amplified regions of genomic DNA injected into the gonads of parents.

Target gene	Number of scored progeny	Affected larvae	%
Non-injected *ok1671*	2656	696	26.2 SD = 2.4
gei-8 rescue after injections	7883	1443	18.3 SD = 3.16

doi:10.1371/journal.pone.0058462.t001

annotations for life span and aging, lipid transport and vitellogenin genes, stress response (heat shock and cellular stress), metabolic genes (sugar metabolism, glycolysis), and neuropeptide signaling (including genes coding for neuropeptide like proteins *nlp-27* to *nlp-32*). The KEGG pathway analysis identified six groups including genes involved in glycolysis (8 genes), cystein methionine metabolism (4 genes), galactose metabolism (3 genes), pentose phosphate pathway (3 genes), fructose and mannose (3 genes) and tryptophan metabolism (3 genes).

One of the most significantly affected genes in the *gei-8(ok1671)* homozygous mutants was Y9C9A.16, encoding a predicted mitochondrial sulfide:quinone oxidoreductase, which had an averaged 7.6-fold increase in expression compared to wild-type controls; this increase was confirmed by RT-qPCR. The Y9C9A.16 region is assayed by Affimetrix probe set 184710_at and, interestingly, includes three 21U-RNAs; 21ur-2020, 21ur-11733 and 21ur-9201. To determine if disruption of expression of Y9C9A.16 affected development, we performed RNAi targeted to the spliced mRNA covered by the Affymetrix probe set (184710_at) or only the regions that include 21ur-2020, 21ur-11733 and 21ur-9201. Progeny of parental animals injected with dsRNA targeting the specific regions were scored using Nomarski optics and fluorescent microscopy (DAPI stained). We were not able to identify any specific phenotype of Y9C9A.16 knockdown in wild type animals. However, because the expression from Y9C9A.16 showed a dramatic response to loss of GEI-8 activity, we thought there might be a biological connection between them. We predicted that knockdown of the expression from Y9C9A.16 locus in *gei-8 (ok1671)* homozygous mutants might revert or modify some of the observed phenotypes; the latter was observed. RNAi-mediated knockdowns targeted to the region covered by the 184710_at probe set and the region containing 21ur-2020, 21ur-11733 and 21ur-9201 induced additional phenotypes in the *gei-8(ok1671)* homozygous mutant background. Additional phenotypes included severe distal tip cell migration defects, irregular gonadal nuclei tumor like accumulation of germline cells and vulval protrusions observed in 13.9% of homozygous *gei-8(ok1671)* animals treated with Y9C9A.16 RNAi (n = 481) (**Figure 6E, F, G, H, I and J and Table 2**). Interestingly, Y9C9A.16 has a paralogue in the *C. elegans* genome, the gene *sqrd-1* (**s**ulfide:**q**uinone oxido**red**uctase). This gene encodes a protein that is identical in size (361 aa) to Y9C9A.16 sharing 266 identical amino acids in its sequence although the genes share very little DNA homology. SQRD-1 expression is regulated by *hif-1* in response to H_2S and HCN [42], is involved in innate immunity and is associated with numerous 21U-RNAs. RNAi targeted to unique regions of the *sqrd-1* coding region, including four 21U-RNAs, resulted in changes in gonad arm migrations and an accumulation of germline cells (4.5% affected, n = 198) that were similar, although less severe, as those observed after Y9C9A.16 RNAi. We concluded that the paralogues encoded by Y9C9A16 and *sqrd-1*, and perhaps their associated 21U-RNAs, have overlapping roles during development of the germline that can be exacerbated by loss of GEI-8 activity.

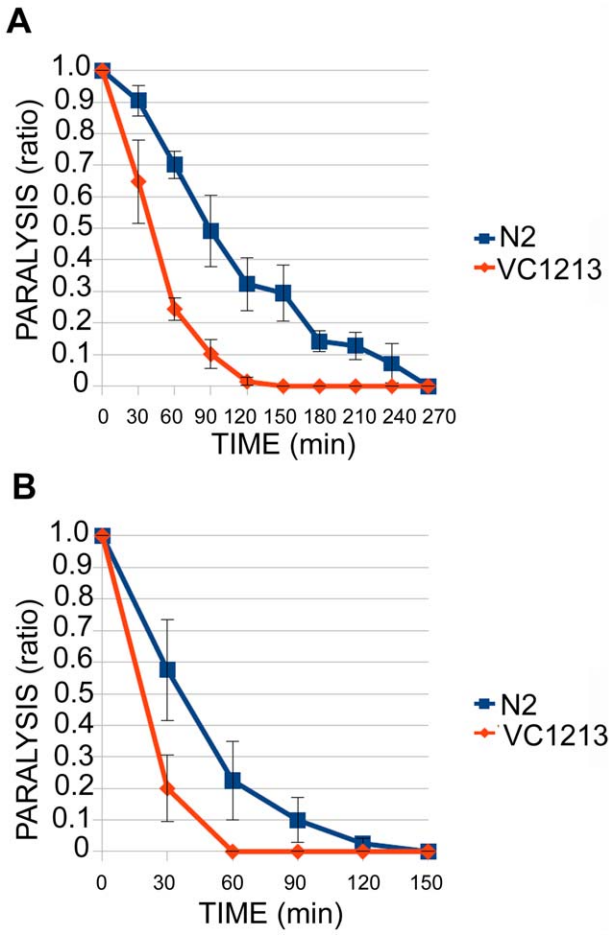

Figure 7. Analysis of neuromuscular function of *gei-8(ok1671)* mutant (VC1213). Aldicarb and levamisole sensitivity assays revealed increased sensitivity of *gei-8* mutants towards the acetylcholinesterase inhibitor aldicarb (**A**) and levamisole (**B**) suggesting a synaptic defect in cholinergic transmission.
doi:10.1371/journal.pone.0058462.g007

Discussion

GEI-8 is a NCoR/SMRT Orthologue with Developmental Roles in *C. elegans*

Our results demonstrate that GEI-8 is the *C. elegans* orthologue of the vertebrate NCoR/SMRT corepressors and that it has essential developmental and transcriptional functions throughout development. GEI-8 has the critical structural motifs necessary for corepressor functions, including the domains for HDAC interaction and activation. Moreover, it is able to interact physically

Table 2. Induction of additional gonad and body shape phenotypes in homozygous *gei-8*(*ok1671*) mutant worms by RNAi directed against *sqrd-2* or *sqrd-1*.

Target gene	Screening method	Hermaphrodites injected	Homozygous larvae scored	Larvae with additional gonad and body shape defects
sqrd-2	Nomarski optics	24	211	40
sqrd-2	DAPI staining	15	270	27
Total for *sqrd-2*	Nomarski optics+DAPI staining	39	481	67 (13.9%)
sqrd-1	Nomarski optics	30	151	5
sqrd-1	DAPI staining	10	47	4
Total for *sqrd-1*	Nomarski optics+DAPI staining	40	198	9 (4.5%)

doi:10.1371/journal.pone.0058462.t002

with nuclear receptors through its C-terminal domain that is known to tether NCoR/SMRT to NRs [21,43,44]. The identification of the NCoR/SMRT homologue in *C. elegans* allows us to extend to invertebrates the conserved developmental functions of these important corepressors. Although such links had been previously suggested by the discovery of SMRTER in *Drosophila*, questions remained because SMRTER was significantly different from the majority of NCoR/SMRT paralogues that had previously been annotated [45]. While the HDAC interacting domain SANT1 is clearly present in *Drosophila* SMRTER (**Figure 1**), the second SANT domain is absent. In this respect, *C. elegans* GEI-8 is more closely related to vertebrate NCoR/SMRT-like NR corepressors than to SMRTER.

We further show that GEI-8 is required for normal development in *C. elegans* based on our studies of a *gei-8* deletion allele that severely truncates or inhibits the protein product. Although expressed, at least at the mRNA level, this mutant allele is predicted to lack the GEI-8 nuclear receptor interacting sites while expressing an mRNA that codes for the domains necessary for HDAC binding and activation. There is no evidence for dominant negative activity of this truncated product as heterozygous animals appear completely wild-type and the introduction of wild-type *gei-8* coding regions in transgenic animals partially rescue multiple mutant phenotypes. Therefore, the mutant phenotypes likely represent the loss of function effects for *gei-8*. Given the early and widespread onset of *gei-8* reporter gene expression in embryos, which is also detected by RT-qPCR, it is very likely that GEI-8 functions throughout development and in most, if not all, tissues. The lack of embryonic or early larval defects in homozygous mutants likely reflects the maternal load of *gei-8* gene products in the embryo. It is also possible that GEI-8 has multiple functions requiring different amount of GEI-8 activity, with demands for higher levels post-embryonically, including germline development.

The most significant phenotype observed in *gei-8* mutants is the late-L4 larval arrest, as revealed by the extent of gonadogenesis and DTC migration. One possibility is that this arrest reflects the depletion of maternally loaded *gei-8* products and that in the absence of GEI-8 activity, development and/or cellular processes fail to be executed properly. This interpretation would be consistent with the late developmental defects seen when other essential, maternally provided gene products are exhausted, such as the G1 cell cycle regulators [46–48]. The second most pronounced phenotype in the *gei-8(ok1671)* homozygous mutants is reduced pharyngeal pumping. It is unclear what defect(s) is responsible for this reduced pharyngeal rate given that it is a semi-autonomous action of the pharyngeal muscles that can be stimulated, but does not require neuronal input [49,50]. One possibility was that food sensation mechanisms were compromised in the *gei-8(ok1671)* mutants; in the absence of food, the pumping rate of wild-type worms is similar to the rate we observed in the homozygous mutants. However, when tested we found that *gei-8(ok1671)* mutants exhibited spontaneous chemotaxis towards OP50 lawns until the mutants terminally arrested late in development demonstrating that food sensation mechanisms were intact. Another explanation of reduced pharyngeal pumping is diminished activity of the MC pharyngeal cholinergic neuron and/or its receptor, EAT-2 that regulate pharyngeal pumping in response to food [51,52]. Such reduced cholinergic signaling is consistent with the sensitivity we observed for *gei-8(ok1671)* mutants to levamisole and aldicarb. Further experiments are needed to determine exactly which pathways are perturbed and the molecular basis for these aberrations.

GEI-8 Regulates Transcription

Whole genome transcriptional analysis indicates that GEI-8 is required for proper gene expression. Its loss-of-function allele resulted in altered expression of a wide range of genes; genes with elevated expression as well as with decreased expression were identified. However, while GO annotation of many genes that showed decreased expression correlated with the observed phenotypes, genes with increased expression (that could be potentially de-repressed) failed to show an obvious correlation. It is interesting to note that among the set of genes that were decreased in mutant worms were several muscle specific genes. Thus, while bodywall muscle was normal by gross observations with normal appearance, there may be defects in this tissue in homozygous mutants.

The set of deregulated (increased) genes included neuropeptide-like protein genes (*nlp-27* to *nlp-32*). The neuropeptides that are generated from these genes fall in the subfamily characterized by the sequence YGGW [53] and are related to Aplysia APGW neuropeptides that regulate male reproductive functions [54]; the functional consequences of this, if any, are currently unknown. However, in agreement with results reported by Yamamoto et al. for mice [13], we have detected numerous metabolic genes in the set of genes with increased expression in homozygous mutant worms.

The set of increased genes included several clusters of metabolic genes involved in lipid transport, sugar metabolism, glycolysis, and amino acid metabolism. Several nuclear receptors may be involved in this metabolic regulation. The majority of *C. elegans*

NRs show similarity to HNF4a but some may support metabolic functions dependent on PPARs in vertebrates, as shown for NHR-49 [55]. Moreover, GEI-8 loss of function may be similar in metabolic regulation as shown for SMRT with a single disabled NR site (ID1 or mRID1, respectively) [56,57]. Interestingly, one of the genes that was increased in *gei-8(ok1671)* mutants (Y9C9A.16) encodes a sulfide:quinone oxidoreductase that we name *sqrd-2*. Our results demonstrate that *sqrd-2* and *gei-8* functions are genetically linked; inhibition of *sqrd-2* in homozygous mutants *gei-8(ok1671)* induces partial reversal of *gei-8* mutant phenotypes as well as additional phenotypic changes. We also demonstrated similar reduction-of-function phenotypes for the *sqrd-2* paralogue, *sqrd-1*. Both *sqrd* genes are associated with 21U-RNAs scattered throughout the non-coding regions. It is intriguing to speculate that the gene expression pattern of *gei-8* loss of function may be dependent on this class of regulatory RNAs. 21U-RNAs have been shown to be critical for sperm development and transposon silencing [58]. Both *sqrd* genes may be linked to their associated non-coding 21U-RNAs that may be localized in mitochondria as part of piRNA biosynthesis [59]. Changes in the mitochondrial compartment induced by *gei-8* inhibition as reported by Yamamoto et al. [13] and observed in our experiments on *gei-8(ok1671)* mutants may also involve piRNAs mediated regulation. The connection to the regulation by 21U-RNAs is supported by our findings that additional changes in the phenotypes of homozygous mutants *gei-8(ok1671)* are induced by RNAi targeted at *sqrd-1* gene. One of the three isoforms of *sqrd-1* is predicted to code for a protein with the same length as the protein derived from *sqrd-2* and both proteins show 74% identity in amino acid sequences suggesting that these proteins may substitute for each other in function. 21U-RNAs located in *sqrd-2* show approximately 50% identity in the conserved cores formed by 16 or 17 bases with piRNAs found in *sqrd-1*. The levels of these non-coding RNAs, like the activity of *sqrd-1* and *-2*, may be critical for gonad and/or germline development and metabolism. The early embryonic lethality of mice lacking NCoR1/SMRT as well as NCoR2 prevents us from assessing whether the role of GEI-8 in gonadogenesis is an evolutionarily conserved feature [3,60]. Interestingly, it was recently found that individual 21U-RNAs are regulated by fork-head transcription factors [61]. Moreover, the fork-head factor FoxP1 regulates development in concert with SMRT [62]. These results raise the intriguing possibility that GEI-8 might be directly involved in the transcriptional regulation of 21U-RNAs.

Materials and Methods

Worm Strains

All strains were maintained as described [63] and were grown on standard NGM plates or, in case of RNA isolation, on NGM plates capped with 2% agarose. Wild-type animals were N2 (var. Bristol). The VC1213 strain, kindly provided by the *C. elegans* Gene Knockout Consortium, carried the *gei-8(ok1671)* allele over a *bli-4* and GFP-marked balancer chromosome; homozygous *gei-8(ok1671)* mutants are lethal. Prior to experiments, we outcrossed the VC1213 strain three times to wild-type males. *gei-8::gfp* transgenic lines were constructed by injecting *gei-8* promoter constructs into N2 hermaphrodites as described previously [64].

Total RNA Isolation and cDNA Preparation

Wild-type *C. elegans* animals were grown on 2% agarose-capped NGM plates, washed with water and frozen at −80°C. After thawing the pellet was resuspended in 0.5 ml of resuspension buffer (0.5% SDS; 5% 2-mercaptoethanol;10 mM EDTA; 10 mM Tris/HCl (pH 7.5) with 15 µl of proteinase K (20 mg/ml)), vortexed for 60 s and incubated at 55°C for 60 min. The sample was phenol-chloroform extracted and ethanol-precipitated, dissolved in water and treated with 1 unit of DNAse (Promega, Madison, WI) per 1 µg of total RNA for 30 min at 37°C. After phenol-chloroform extraction and ethanol-precipitation RNA was resuspended in DEPC water. cDNA was synthesized from the isolated RNA using Roche Transcriptor High Fidelity cDNA Synthesis Kit (Roche, Basel, Switzerland) with poly-T and gene specific primer 6242 from the 3′ untranslated region (UTR) of *gei-8*, or using Superscript II kit (Invitrogen, Carlsbad, CA) with random hexamer primers, all according to protocols by manufacturers.

RNA Interference

Y9C9A.16 dsRNA was synthesized using a 774 bp region of gDNA containing exons 2 to 6 amplified by primers 7501 and 7502 and cloned into pCRII vector (Invitrogen). Prior to in-vitro transcription by T7 or Sp6 polymerases, the construct was linearized. dsRNA was prepared by incubating ssRNAs at 70°C for 10 min and at 37°C for 30 min, followed by phenol-chloroform purification, ethanol-precipitation and dilution in DEPC water. dsRNA was injected into gonads of N2 wild-type hermaphrodites, heterozygous *gei-8(ok1671)* mutants, and homozygous wild-type progeny of heterozygous *gei-8(ok1671)* mutant parents. *sqrd-1* RNAi was prepared as mentioned above using primers 7605 and 7606.

Immunostaining

L4 stage homozygous VC1213 mutants and N2 control animals were put on slides coated with poly-L-lysine, fixed in 5% paraformaldehyde, covered by a cover glass and incubated in a wet chamber for 30 minutes at room temperature. Freeze crack was performed after freezing the sample on dry ice for 5 minutes. Samples were placed in −20°C methanol followed by series of rehydration in methanol:TTBS (9:1, 7:3, 1:1 and 1:4 10 minutes each). Staining of actin filaments was done using phalloidin labeled with Alexa Fluor 488 (Molecular Probes, Eugene, OR). Samples were incubated with phalloidin (1:500 dilution) for 40 min and then washed in TTBS three times. Samples were mounted with fluorescent mounting medium (DakoCytomation, Copenhagen, Denmark) and coated with nail polish.

Immunostaining of myosin filaments was performed using anti-MYO3 antibody [65]. After rehydration samples were incubated with anti-MYO3 mouse antibody (1:200 dilution) for 24 hours at 4°C, then incubated with anti-mouse IgG antibody labeled with Alexa Fluor 568 (1:400 dilution). Each incubation with antibody was followed by three TTBS washes. Samples were mounted as described above.

Staining with 4′,6-diamidino-2-phenylindole (DAPI)

L4 stage homozygous *gei-8(ok1671)* mutants and N2 control animals selected from progeny of injected mothers were put on slides coated with poly-L-lysine and 20 µl of water, covered by a cover glass and put on dry ice. Freeze crack was performed after freezing the sample on dry ice for 5 minutes. Samples were kept in −20°C methanol for 10 minutes, then stained with DAPI (20 µl, 1:1000 dilution of 1 mg/ml) and mounted with fluorescent mounting medium (DakoCytomation, Copenhagen, Denmark) and coated with nail polish.

Longevity Assays

Longevity assays were performed as described [66] with modification. Adult hermaphrodites were allowed to lay eggs for 4–5 hours. Homozygous *gei-8(ok1671* mutants (n = 21) and N2 controls (n = 12) were cultured at 20°C and transferred to a new plate every second day. The vitality of the animals was checked once per day. Death was defined as cessation of pharyngeal pumping or lack of response to prodding.

Cloning

We used primers designed according to predicted sequences of *gei-8* isoforms *a*, *b* and *c* (WormBase WS195). Multiple regions were amplified by Accuprime polymerase (Invitrogen), cloned into TOPO pCRII, pCR4 or XL vectors (Invitrogen) and sequenced (Avant 3100). Selected clones are displayed in **Figure 2A and C**. Primer sequences are as follows: 107, 7149, 7144, and 6242. The sequences of all primers are in **Table S3**.

Sequencing the *gei-8(ok1671)* Allele

The mutation in strain VC1213 was confirmed by single-worm PCR with primers 107 and 307 producing bands of expected sizes for mutant and wild-type worms. The nature of *gei-8(ok1671)* deletion was confirmed by sequencing these PCR fragments (Avant 3100).

Aldicarb and Levamisole Sensitivity Assays

L4 *gei-8(ok1671)* homozygous mutants and L4 N2 wild-type animals were scored for aldicarb or levamisole sensitivity on NGM plates with 1 mM aldicarb [38] or 1 mM levamisole [39]. The assays were performed at room temperature and scored every 30 minutes until complete paralysis of all animals. Paralysis was defined as cessation of pharyngeal pumping and lack of response to prodding. The score was plotted as the ratio of moving animals to the total number of all animals on the plate.

Locomotion Assays

Thrashing assays were performed in 15 µl of 1× PBS solution on non-adhesive slides. One thrash was defined as a complete swing of the head, for example from left to right and left again. L4 stage VC1213 mutant animals and N2 controls were compared. All worms were allowed to acclimate to the solution for one min prior to scoring. The total number of thrashes was counted in one minute intervals. The pharyngeal pumping rate was counted per minute in well-fed worms in the presence of food at 20°C and VC1213 and N2 controls were compared at the L2, L3 and L4 stages (n = 10 for each stage).

Real-time PCR

Two regions of the *gei-8* gene were analyzed for expression using the LightCycler 480 and the LightCycler® 480 SYBR Green I Master kit (Roche Diagnostics, Basel, Switzerland). Region 1 was amplified by primers 6200 and 05/153. Region 2 was amplified by primers 6168 and 01/042. We performed two independent reactions for each region. Reaction conditions were as follows: 5 min pre-denaturation at 95°C followed by 45 cycles amplification (10 s at 95°C, 15 s at 59°C, 15 s at 72°C) and melting curve analyses (5 s at 95°C, 1 min at 65°C and then continuously increasing temperature up to 97°C (temp rate 0,2°C/s)). Data were processed by the LightCycler® 480 software version 1.5. Efficiency values reflected standard curve dilution series, which corresponded to gel-purified ethanol-precipitated PCR products. The Cp values of studied genes were normalized relative to the constitutive gene *ama-1* encoding the large subunit of RNA polymerase II [67,68].

Mutant Rescue

The *gei-8* promoter and coding sequence was amplified in two overlapping PCR products RES1 and RES2 with primers 6174 and 6173; 6158 and 6243, respectively. The size of the overlapping region was 191 bp. Both PCR products were mixed together to a final concentration 250 ng/µl and injected with the pRF4 *(rol-6(su1006))* dominant marker at 100 ng/µl in VC1213 mutant or wild-type adult hermaphrodites. Rollers were selected from the progeny of injected mothers and kept individually per plate at 16°C until they finished laying eggs. Total progeny were counted and scored for embryonic lethality and the number animals carrying the mutant phenotype [31–34].

GFP Reporters

Transgenic lines expressing *gei-8::gfp* from putative promoter 1 contains 1832 bp upstream of the translational start codon and 222 bp of predicted exon 1 of *gei-8b* and *c*. Putative promoter 2 contains 2300 bp upstream of ATG. Promoter 1 was amplified using primers 01/021 and 4938. Promoter 2 was amplified using primers 5056 and 5060. Promoter fragments were cloned into the GFP vectors pPD95.69 and pPD95.67, respectively and injected into L4 hermaphrodites. Both constructs contained a nuclear localization signal.

Transgenic lines expressing *gei-8::gfp* from putative promoter 3 were created by a PCR fusion-based approach described by Hobert (2002). A 6.2 kb long putative promoter region of *gei-8* was amplified by primers 6228 and 6230. Primer 6230 contains an overhang complementary to the *gfp* sequence of the pPD95.75 vector. The second product, containing *gfp* and *unc-54* sequences was amplified by standard primers 6232 and 6233 using the pPD95.75 vector as template. The overlapping fusion PCR product was obtained by diluting the two products with water to 10–50 ng/µl and using a 1:1 mixture as a template for a subsequent PCR reaction with nested primers 6229 and 6234. The PCR fusion product was diluted to a final concentration of 50 ng/µl, mixed with the injection marker *rol-6* at 50 ng/µl and injected in N2 adult hermaphrodite animals. GFP expression was selected for until stable expressing lines were established.

Microarrays

C. elegans whole genome expression microarrays (Affymetrix, Santa Clara, CA) were used to profile gene expression in three independent replicates based on manually selected homozygous *gei-8(ok1671)* mutants and matched N2 wild-type larvae at the earliest stage when mutants can be easily recognized based on their movement phenotype. Microarray chip data was analyzed by Affymetrix MAS 5.0 suite software (1.6-fold change in mRNA expression) and Robust Multichip Average (RMA) (1.2-fold change in mRNA expression) as part of the Partek genomics suite software package, all with a p-value less than or equal to 0.05. The microarray data has been deposited in the NCBI's GEO database (http://www.ncbi.nlm.nih.gov/geo) accession number GSE40127.

Detection of Mitochondrial Activity by MitoTracker Labeling

Manually selected worms were transferred to a 10 µl drop of 10 µM MitoTracker Red CMXRos (Invitrogen, Molecular Probes) for 2 hr at room temperature (21°C) in PBS and were kept in dark. Worms were transferred in a drop of 20 µl PBS to

NGM plate seeded with OP50 bacteria and kept in dark for 2 hr. Worms were then manually transferred to microscopic slides with agarose layer for fluorescent microscopy. For densitometric analysis, L4 larvae were analyzed using the Olympus BX60 microscope with a DP30 camera and pictures recorded at constant settings. For densitometric analysis, pictures of 12 larvae were used (four for each group, N2 wild-type larvae, mutant larvae *gei-8(ok1671)* determined by their moving phenotype and worms from the progeny of heterozygous *gei-8(ok1761)* that appeared normal). The total area of 149 000 μm^2 was analyzed in total 40 selected areas (excluding areas for determination of background values) using the computer program ImageJ Version 1.42q (Rasband, W.S., ImageJ, U. S. National Institutes of Health, Bethesda, Maryland, USA, http://imagej.nih.gov/ij/, 1997–2011).

GST Pull-down Assay

The complete coding cDNA of NHR-60 [24] (with the exception of the first methionine codon) was amplified by PCR using primers 10/44 and 10/45 and cloned in pGEX-2T vector (Amersham Pharmacia Biotech, Amersham, UK). The glutathione-S-transferase (GST) fusion protein was expressed in *Escherichia coli* (BL-21-strain). For control experiments, the protein domain of GST was expressed from the pGEX-2T empty vector. Overnight cultures of transformed bacteria obtained from a single bacterial colony were cultured in 400 ml of Luria-Broth culture medium containing 100 μg/ml ampicillin at 37°C overnight. Cultures with O. D. (600 nm) = 0.8 were induced using 1 mM isopropylthiogalactopyranoside (IPTG) and the cultures were cultivated at 20°C for an additional 5 hr prior to harvesting by centrifugation at 3300×g in a swing out rotor at 4°C for 10 min. The bacteria were washed twice in phosphate-buffered saline (PBS) and resuspended in 5 ml of PBS. Bacteria were lysed in 6 ml of Lysis buffer, (Bio-Rad Laboratories, Hercules, CA) supplemented with protease inhibitor (1× COMPLETE, Roche, Basel, Switzerland), incubated on ice for 10 minutes with intermittent vortexing and sonicated four times 10 sec. at 80% intensity (Sonicator UP100H, Hielscher Ultrasonics, Teltow, Germany). The lysates were centrifugated at 11180×g/4°C/10 min. The supernatant was removed and filtered using a 0.22 μm filter. Glutathione-agarose (Sigma-Aldrich, Saint Louis, MO) was prepared by swelling 0.01 g of beads in 1 ml PBS (137 mM NaCl, 2.7 mM KCl, 4.3 mM Na2HPO4, 1.45 mM KH2PO4, pH 7.5). The beads were collected by sedimentation and swelling completed by repeating the swelling step for an additional 5 min. The beads were then resuspended in 100 ul of PBS. The resulting slurry was used for binding of GST or GST-NHR-60. For purification of GST-NHR-60 and GST, 100 μl of slurry (containing 0.01 g of beads), and 300 μl of bacterial lysates were incubated for 30 minutes at 4°C with intermittent mixing (approximately every 4 minutes). The beads were washed four times in 1 ml of PBS Triton X-100 (1%) (Sigma-Aldrich, Saint Louis, MO). Beads were collected by sedimentation and resuspended in 500 μl of PBS. The resulting slurry was divided to four aliquots of 100 μl that were used for the binding assay.

The C-terminal domains of *gei-8a* coding for regions with the putative NR binding sites were amplified by PCR from cDNA and cloned in three constructs in pCR4 or pCRII TOPO-TA cloning vectors (Invitrogen, Carlsbad, CA). The three constructs marked as I, II, III were prepared using the following primers and positions in *gei-8a* isoform (Construct I: 7749, 7750; position 2480–3485, construct II: 7751, 7752; position 3413–4389; construct III: 7753, 7754; position 4274–5513). Constructs I and III included the predicted NR sites, NR1 and NR2 respectively.

^{35}S-radiolabeled proteins were prepared using an in-vitro TNT T7/T3 coupled reticulocyte lysate system (Promega, Madison, WI) and 1.48 MBq of ^{35}S-methionine (37 TBq/mmol) (Institute of Isotopes, Budapest, Hungary) in the final volume 50 μl. Ten microliters of the final TNT product was used for binding at 22°C for 30 minutes with intermittent mixing every 4 minutes. The beads were washed 3 times in 1 ml of PBS and resuspended in a final volume of 40 μl of PBS. Subsequently 5 μl of 2 × Laemmli Buffer and 1 μl of beta-mercaptoethanol were added, samples were boiled for 5 minutes and 25 μl were used for polyacrylamide gel electrophoresis and autoradiography. 10 μl of supernatant was used for determination of ^{35}S-methionine in samples using the Liquid Scintillation Analyzer Tri-Carb 1600 TR (Packard, Meriden, CT) and Ultima-Gold scintillation cocktail (Perkin Elmer, Waltham, MA). For determination of input in binding experiments, 2 μl of in-vitro transcribed-translated product was resolved using polyacrylamide gel electrophoresis, transferred on Whitman 3M paper, dried and radioactivity determined in cut stripes containing the translated proteins but not the unincorporated ^{35}S-methionine.

Supporting Information

Figure S1 Binding analysis of C-terminal domains of GEI-8 including the predicted NR binding sites to GST-NHR-60. (A). Pull-down experiment of GST (lanes 1 to 3) and GST-NHR-60 (lanes 4 to 6) with in vitro translated proteins covering the C-terminal domains of GEI-8 (GEI-8*) cloned in three constructs: domain I (position 2480–3485 in *gei-8a*, lanes 1 and 4), domain II (position 3413–4389) lanes 2 and 5 and domain III (position 4274–5513) lanes 3 and 6. The domains I and III contain the predicted NR1 and NR2 binding sites, respectively. (B) Pulled-down radioactivity determined by scintillation detection in the fractions shown in panel A. GST-NHR-60 binds in vitro translated domain I of GEI-8 (lane 4 in panel A and the corresponding bar in panel B) supporting the functional similarity between GEI-8 C-terminal region and NCoR/SMRT. The figure presents one of two experiments that gave similar results.
(PDF)

Figure S2 Elevated mitochondrial activity in mutant *gei-8(ok1671)* larvae. Control wild-type N2 L4 larvae and progeny of heterozygous mutant in the same developmental stage were stained using MitoTracker staining as described (Materials and methods). Panels A, D, G, and J show N2 control animals; panels B, E, H, and K show progeny of a mutant heterozygous parent that lack the mutant phenotype and represent heterozygous or wild-type larvae; panels C, F, I and L show homozygous mutant larvae, from the same parent. Exposure time was 50 ms in panels A, B and C and 100 ms in all other panels. Panels A to F show the proximal part of larvae; panels G to I show the middle part of the larval bodies and panels J to L show the distal part of larvae. Elevated activity in homozygous animals is apparent in panels C, F, I and L. The scale bar represents 100 μm.
(PDF)

Figure S3 Densitometric analysis of MitoTracker staining expressed in arbitrary units. N2 wild-type animals, and the progeny of heterozygous mutant parents divided according to the mutant phenotype to phenotypically normal heterozygous (+/−) and phenotypically homozygous (−/−) animals were analyzed. Elevated staining by MitoTracker in homozygous mutant larvae is statistically significant in paired Student's T-test compared to both N2 and morphologically unaffected progeny of heterozygous parents ($p<0.01$).

(PDF)

Table S1 List of genes with decreased expression in *gei-8(ok1671)* homozygous mutants.
(PDF)

Table S2 List of genes with increased expression in *gei-8(ok1671)* homozygous mutants.
(PDF)

Table S3 Primers used in the study.
(PDF)

Acknowledgments

We thank Dr. A. Fire for GFP and L4440 vectors and the bacterial strain used in RNAi.

Author Contributions

Editing, revising and approving of the manuscript: PM VS Markéta Kostrouchová MWK ZK Marta Kostrouchová. Conceived and designed the experiments: PM MWK ZK Marta Kostrouchová. Performed the experiments: PM JK KS PY Markéta Kostrouchová MWK ZK Marta Kostrouchová. Analyzed the data: PM JK KS PY Markéta Kostrouchová VS MWK ZK Marta Kostrouchová. Contributed reagents/materials/analysis tools: PM MWK ZK Marta Kostrouchová. Wrote the paper: PM VS Markéta Kostrouchová MWK ZK Marta Kostrouchová.

References

1. Horlein AJ, Naar AM, Heinzel T, Torchia J, Gloss B, et al. (1995) Ligand-independent repression by the thyroid hormone receptor mediated by a nuclear receptor co-repressor. Nature 377: 397–404.
2. Chen JD, Evans RM (1995) A transcriptional co-repressor that interacts with nuclear hormone receptors. Nature 377: 454–7.
3. Jepsen K, Hermanson O, Onami TM, Gleiberman AS, Lunyak V, et al. (2000) Combinatorial roles of the nuclear receptor corepressor in transcription and development. Cell 102: 753–63.
4. Goodson M, Jonas BA, Privalsky MA (2005) Corepressors: custom tailoring and alterations while you wait. Nucl Recept Signal 3: e003.
5. Ogata K, Morikawa S, Nakamura H, Sekikawa A, Inoue T, et al. (1994) Solution structure of a specific DNA complex of the Myb DNA-binding domain with cooperative recognition helices. Cell 79: 639–48.
6. Tahirov TH, Sasaki M, Inoue-Bungo T, Fujikawa A, Sato K, et al. (2001) Crystals of ternary protein-DNA complexes composed of DNA-binding domains of c-Myb or v-Myb, C/EBPalpha or C/EBPbeta and tom-1A promoter fragment. Acta Crystallogr D Biol Crystallogr 57: 1655–8.
7. Boyer LA, Latek RR, Peterson CL (2004) The SANT domain: a unique histone-tail-binding module? Nat Rev Mol Cell Biol 5: 158–63.
8. Yu J, Li Y, Ishizuka T, Guenther MG, Lazar MA (2003) A SANT motif in the SMRT corepressor interprets the histone code and promotes histone deacetylation. Embo J 22: 3403–10.
9. Guenther MG, Barak O, Lazar MA (2001) The SMRT and N-CoR corepressors are activating cofactors for histone deacetylase 3. Mol Cell Biol 21: 6091–101.
10. Codina A, Love JD, Li Y, Lazar MA, Neuhaus D, et al. (2005) Structural insights into the interaction and activation of histone deacetylase 3 by nuclear receptor corepressors. Proc Natl Acad Sci U S A 102: 6009–14.
11. Ahringer J (2000) NuRD and SIN3 histone deacetylase complexes in development. Trends Genet 16: 351–6.
12. Choy SW, Wong YM, Ho SH, Chow KL (2007) C. elegans SIN-3 and its associated HDAC corepressor complex act as mediators of male sensory ray development. Biochem Biophys Res Commun 358: 802–7.
13. Yamamoto H, Williams EG, Mouchiroud L, Canto C, Fan W, et al. (2011) NCoR1 is a conserved physiological modulator of muscle mass and oxidative function. Cell 147: 827–39.
14. Tsuboi D, Qadota H, Kasuya K, Amano M, Kaibuchi K (2002) Isolation of the interacting molecules with GEX-3 by a novel functional screening. Biochem Biophys Res Commun 292: 697–701.
15. Hodgson MC, Shen HC, Hollenberg AN, Balk SP (2008) Structural basis for nuclear receptor corepressor recruitment by antagonist-liganded androgen receptor. Mol Cancer Ther 7: 3187–94.
16. Altschul SF, Madden TL, Schaffer AA, Zhang J, Zhang Z, et al. (1997) Gapped BLAST and PSI-BLAST: a new generation of protein database search programs. Nucleic Acids Res 25: 3389–402.
17. Biegert A, Mayer C, Remmert M, Soding J, Lupas AN (2006) The MPI Bioinformatics Toolkit for protein sequence analysis. Nucleic Acids Res 34: W335–9.
18. Birney E, Clamp M, Durbin R (2004) GeneWise and Genomewise. Genome Res 14: 988–95.
19. Kemena C, Notredame C (2009) Upcoming challenges for multiple sequence alignment methods in the high-throughput era. Bioinformatics 25: 2455–65.
20. Ogawa S, Lozach J, Jepsen K, Sawka-Verhelle D, Perissi V, et al. (2004) A nuclear receptor corepressor transcriptional checkpoint controlling activator protein 1-dependent gene networks required for macrophage activation. Proc Natl Acad Sci U S A 101: 14461–6.
21. Hu X, Li Y, Lazar MA (2001) Determinants of CoRNR-dependent repression complex assembly on nuclear hormone receptors. Mol Cell Biol 21: 1747–58.
22. Malartre M, Short S, Sharpe C (2004) Alternative splicing generates multiple SMRT transcripts encoding conserved repressor domains linked to variable transcription factor interaction domains. Nucleic Acids Res 32: 4676–86.
23. Michelitsch MD, Weissman JS (2000) A census of glutamine/asparagine-rich regions: implications for their conserved function and the prediction of novel prions. Proc Natl Acad Sci U S A 97: 11910–5.
24. Simeckova K, Brozova E, Vohanka J, Pohludka M, Kostrouch Z, et al. (2007) Supplementary nuclear receptor NHR-60 is required for normal embryonic and early larval development of Caenorhabditis elegans. Folia Biol (Praha) 53: 85–96.
25. Torres-Padilla ME, Sladek FM, Weiss MC (2002) Developmentally regulated N-terminal variants of the nuclear receptor hepatocyte nuclear factor 4alpha mediate multiple interactions through coactivator and corepressor-histone deacetylase complexes. J Biol Chem 277: 44677–87.
26. Celniker SE, Dillon LA, Gerstein MB, Gunsalus KC, Henikoff S, et al. (2009) Unlocking the secrets of the genome. Nature 459: 927–30.
27. MacMorris M, Kumar M, Lasda E, Larsen A, Kraemer B, et al. (2007) A novel family of C. elegans snRNPs contains proteins associated with trans-splicing. Rna 13: 511–20.
28. Hobert O (2002) PCR fusion-based approach to create reporter gene constructs for expression analysis in transgenic C. elegans. Biotechniques 32: 728–30.
29. Kelly WG, Xu S, Montgomery MK, Fire A (1997) Distinct requirements for somatic and germline expression of a generally expressed Caernorhabditis elegans gene. Genetics 146: 227–38.
30. Barberan-Soler S, Lambert NJ, Zahler AM (2009) Global analysis of alternative splicing uncovers developmental regulation of nonsense-mediated decay in C. elegans. Rna 15: 1652–60.
31. Maryon EB, Coronado R, Anderson P (1996) unc-68 encodes a ryanodine receptor involved in regulating C. elegans body-wall muscle contraction. J Cell Biol 134: 885–93.
32. Maryon EB, Saari B, Anderson P (1998) Muscle-specific functions of ryanodine receptor channels in Caenorhabditis elegans. J Cell Sci 111 (Pt 19): 2885–95.
33. Mercer KB, Flaherty DB, Miller RK, Qadota H, Tinley TL, et al. (2003) Caenorhabditis elegans UNC-98, a C2H2 Zn finger protein, is a novel partner of UNC-97/PINCH in muscle adhesion complexes. Mol Biol Cell 14: 2492–507.
34. Watanabe N, Nagamatsu Y, Gengyo-Ando K, Mitani S, Ohshima Y (2005) Control of body size by SMA-5, a homolog of MAP kinase BMK1/ERK5, in C. elegans. Development 132: 3175–84.
35. Faumont S, Miller AC, Lockery SR (2005) Chemosensory behavior of semi-restrained Caenorhabditis elegans. J Neurobiol 65: 171–8.
36. Han HF, Beckerle MC (2009) The ALP-Enigma protein ALP-1 functions in actin filament organization to promote muscle structural integrity in Caenorhabditis elegans. Mol Biol Cell 20: 2361–70.
37. Glenn CF, Chow DK, David L, Cooke CA, Gami MS, et al. (2004) Behavioral deficits during early stages of aging in Caenorhabditis elegans result from locomotory deficits possibly linked to muscle frailty. J Gerontol A Biol Sci Med Sci 59: 1251–60.
38. Mahoney TR, Luo S, Nonet ML (2006) Analysis of synaptic transmission in Caenorhabditis elegans using an aldicarb-sensitivity assay. Nat Protoc 1: 1772–7.
39. Gottschalk A, Almedom RB, Schedletzky T, Anderson SD, Yates JR 3rd, et al. (2005) Identification and characterization of novel nicotinic receptor-associated proteins in Caenorhabditis elegans. Embo J 24: 2566–78.
40. Huang D, Sherman BT, Lempicki RA (2009) Systematic and integrative analysis of large gene lists using DAVID bioinformatics resources. Nat Protoc 4: 44–57.
41. Arakawa K, Kono N, Yamada Y, Mori H, Tomita M (2005) KEGG-based pathway visualization tool for complex omics data. In Silico Biol 5: 419–23.
42. Budde MW, Roth MB The response of Caenorhabditis elegans to hydrogen sulfide and hydrogen cyanide. Genetics 189: 521–32.
43. Cohen RN, Brzostek S, Kim B, Chorev M, Wondisford FE, et al. (2001) The specificity of interactions between nuclear hormone receptors and corepressors is mediated by distinct amino acid sequences within the interacting domains. Mol Endocrinol 15: 1049–61.
44. Privalsky ML (2001) Regulation of SMRT and N-CoR corepressor function. Curr Top Microbiol Immunol 254: 117–36.

45. Tsai CC, Kao HY, Yao TP, McKeown M, Evans RM (1999) SMRTER, a Drosophila nuclear receptor coregulator, reveals that EcR-mediated repression is critical for development. Mol Cell 4: 175–86.
46. Park M, Krause MW (1999) Regulation of postembryonic G(1) cell cycle progression in Caenorhabditis elegans by a cyclin D/CDK-like complex. Development 126: 4849–60.
47. Fay DS, Han M (2000) Mutations in cye-1, a Caenorhabditis elegans cyclin E homolog, reveal coordination between cell-cycle control and vulval development. Development 127: 4049–60.
48. Boxem M, van den Heuvel S (2001) lin-35 Rb and cki-1 Cip/Kip cooperate in developmental regulation of G1 progression in C. elegans. Development 128: 4349–59.
49. Avery L, Horvitz HR (1989) Pharyngeal pumping continues after laser killing of the pharyngeal nervous system of C. elegans. Neuron 3: 473–85.
50. Albertson DG, Thomson JN (1976) The pharynx of Caenorhabditis elegans. Philos Trans R Soc Lond B Biol Sci 275: 299–325.
51. McKay JP, Raizen DM, Gottschalk A, Schafer WR, Avery L (2004) eat-2 and eat-18 are required for nicotinic neurotransmission in the Caenorhabditis elegans pharynx. Genetics 166: 161–9.
52. Raizen DM, Lee RY, Avery L (1995) Interacting genes required for pharyngeal excitation by motor neuron MC in Caenorhabditis elegans. Genetics 141: 1365–82.
53. Nathoo AN, Moeller RA, Westlund BA, Hart AC (2001) Identification of neuropeptide-like protein gene families in Caenorhabditiselegans and other species. Proc Natl Acad Sci U S A 98: 14000–5.
54. Fan X, Croll RP, Wu B, Fang L, Shen Q, et al. (1997) Molecular cloning of a cDNA encoding the neuropeptides APGWamide and cerebral peptide 1: localization of APGWamide-like immunoreactivity in the central nervous system and male reproductive organs of Aplysia. J Comp Neurol 387: 53–62.
55. Van Gilst MR, Hadjivassiliou H, Jolly A, Yamamoto KR (2005) Nuclear hormone receptor NHR-49 controls fat consumption and fatty acid composition in C. elegans. PLoS Biol 3: e53.
56. Yu C, Markan K, Temple KA, Deplewski D, Brady MJ, et al. (2005) The nuclear receptor corepressors NCoR and SMRT decrease peroxisome proliferator-activated receptor gamma transcriptional activity and repress 3T3-L1 adipogenesis. J Biol Chem 280: 13600–5.
57. Fang S, Suh JM, Atkins AR, Hong SH, Leblanc M, et al. (2010) Corepressor SMRT promotes oxidative phosphorylation in adipose tissue and protects against diet-induced obesity and insulin resistance. Proc Natl Acad Sci U S A 108: 3412–7.
58. Batista PJ, Ruby JG, Claycomb JM, Chiang R, Fahlgren N, et al. (2008) PRG-1 and 21U-RNAs interact to form the piRNA complex required for fertility in C. elegans. Mol Cell 31: 67–78.
59. Huang H, Gao Q, Peng X, Choi SY, Sarma K, et al. (2011) piRNA-associated germline nuage formation and spermatogenesis require MitoPLD profusogenic mitochondrial-surface lipid signaling. Dev Cell 20: 376–87.
60. Jepsen K, Solum D, Zhou T, McEvilly RJ, Kim HJ, et al. (2007) SMRT-mediated repression of an H3K27 demethylase in progression from neural stem cell to neuron. Nature 450: 415–9.
61. Cecere G, Zheng GX, Mansisidor AR, Klymko KE, Grishok A (2012) Promoters recognized by forkhead proteins exist for individual 21U-RNAs. Mol Cell 47: 734–45.
62. Jepsen K, Gleiberman AS, Shi C, Simon DI, Rosenfeld MG (2008) Cooperative regulation in development by SMRT and FOXP1. Genes Dev 22: 740–5.
63. Brenner S (1974) The genetics of Caenorhabditis elegans. Genetics 77: 71–94.
64. Fire A, Xu S, Montgomery MK, Kostas SA, Driver SE, et al. (1998) Potent and specific genetic interference by double-stranded RNA in Caenorhabditis elegans. Nature 391: 806–11.
65. Fire A, Waterston RH (1989) Proper expression of myosin genes in transgenic nematodes. Embo J 8: 3419–28.
66. Lakowski B, Hekimi S (1998) The genetics of caloric restriction in Caenorhabditis elegans. Proc Natl Acad Sci U S A 95: 13091–6.
67. Kostrouchova M, Krause M, Kostrouch Z, Rall JE (2001) Nuclear hormone receptor CHR3 is a critical regulator of all four larval molts of the nematode Caenorhabditis elegans. Proc Natl Acad Sci U S A 98: 7360–5.
68. Dorak MT (2006) Real-time PCR (Advanced Methods) (Routledge, UK, Abingdon).